Cross Sections and Rate Coefficients for the Interaction of a Monoenergetic Neutral Lithium Beam with a Maxwellian Plasma

K. McCormick

IPP III/40 January 1978

MAX-PLANCK-INSTITUT FÜR PLASMAPHYSIK

8046 GARCHING BEI MÜNCHEN

MAX-PLANCK-INSTITUT FÜR PLASMAPHYSIK

GARCHING BEI MÜNCHEN

Cross Sections and Rate Coefficients for the Interaction of a Monoenergetic Neutral Lithium Beam with a Maxwellian Plasma

K. McCormick

IPP III/40 January 1978

Die nachstehende Arbeit wurde im Rahmen des Vertrages zwischen dem Max-Planck-Institut für Plasmaphysik und der Europäischen Atomgemeinschaft über die Zusammenarbeit auf dem Gebiete der Plasmaphysik durchgeführt.

Table of Contents

IPP III/40 K.McCormick

Cross sections and rate coefficients for the interaction of a monoenergetic neutral lithium beam with a Maxwellian plasma.

Abstract

Cross sections and rate coefficients for the interaction of a monoenergetic neutral lithium beam with a Maxwellian plasma are presented. Experimentally determined cross sections from the literature are used for the ionization of lithium atoms by electron impact and by charge exchange on protons as well as for the excitation of the Li(2s-2p) line by electrons. The analytical expressions of Gryzinski /1/ are employed to compute the cross sections for the ionization of lithium by ions and for the excitation of the Li(2s-2p) line by ions. The calculations are done for electron and proton temperatures in the range 10 eV to 10 keV with the lithium beam energy being varied as a parameter between 4 and 100 keV.

List of Symbols and Frequently Used Constants

$N_{h\nu}$	Number of photons emitted per cm^3 per second in 4π sterradians, at a distance ℓ into the plasma, as a result of line excitation by collisional interaction of plasma particles with the atoms in a neutral beam
E_b	Lithium beam energy
E_e, E_i, E_p	Kinetic energy of bombarding electron, ion and proton
e	Electronic charge = 1.6021×10^{-19} Coulomb
m_e	Electron mass = 9.1095×10^{-31} kg
m_i	Ion mass
m_p	Proton mass = 1.6726×10^{-27} kg
m_{Li}	Atomic lithium mass = 6.94 a.m.u. = 1.153×10^{-26} kg
M_i	Ion mass in atomic mass units 1 a.m.u = 1.6606×10^{-27} kg
n_j	Density $[cm^{-3}]$ of the j^{th} plasma species
n_e, n_i, n_p	Electron, ion and proton density $[cm^{-3}]$

n^o_{Li} Density of lithium atoms in beam for the case of no beam attenuation

$$= 3.743 \times 10^{11} \frac{J_b\,[A/cm^2]}{E_b^{1/2}\,[keV]} \quad cm^{-3}$$

J_b Beam equivalent current density = $n^o_{Li}\, v_b e$

v_b Beam velocity $= 4.393 \times 10^7 \frac{E_b^{1/2}\,[keV]}{M_i^{1/2}\,[a.m.u.]}$ cm/s

$= 1.667 \times 10^7 E_b^{1/2}\,[keV]$ cm/s for Li

$\vec{v}$ Plasma particle velocity

$\vec{v}_r$ Relative velocity between the interacting plasma particle under consideration and the beam, $\vec{v}_r = \vec{v} - \vec{v}_b$

w Root-mean-square speed of an ensemble of particles each of mass m having a Maxwellian velocity distribution characterized by a temperature kT,

$$w = \sqrt{\frac{2\ kT}{m}} = \sqrt{\frac{2e\ T_k}{m_k}}$$

T_e, T_i, T_p Temperature [eV] of the electrons, ions and protons constituting the plasma

${}_j\sigma^k$ Cross section for the k^{th} process (ionization, k=i; charge-exchange, k=cx; Li(2s-2p) excitation, k=exc) by the j^{th} species (electrons, j=e; ions, j=i; protons, j=p)

${}_j\langle\sigma v\rangle^k$ Rate coefficient for the k^{th} process by the j^{th} species

${}_j\sigma^k_{eff}$ Effective cross section = $\frac{{}_j\langle\sigma v\rangle^k}{v_b}$

σ_T Total cross section for beam attenuation

$$= \frac{1}{n_e} \sum_{j,k} n_j \; {}^{k}_{j}\sigma_{eff}$$

σ_o $= 6.56 \times 10^{-14}$ eV cm^2

σ_o' $= Z_i^2 \, \sigma_o$

Z_i Ionic charge in units of the electronic charge

Z_{eff} Effective ionic charge of plasma for Coulomb interactions

$$= \sum_j n_j Z_j^2 \Big/ \sum n_j Z_j = \frac{1}{n_e} \sum_j n_j Z_j^2$$

χ, χ_r, χ_b $= v/w, \; v_r/w, \; v_b/w$

U_{exc} Li(2s-2p) excitation energy = 1.85 eV

U_i Binding energy of the orbital electron in the i^{th} shell of a neutral atom
For lithium: U_{2s}= 5.39 eV; U_{1s}= 55 eV

x $= E_e/U_i$

x' $= \frac{m_e}{m_i} \; \frac{E_e}{U_i}$

y $= U_{exc}/U_i$ = .343 for Li(2s-2p)

1. Introduction

With the advent of the neutral lithium beam as a diagnostic tool /2,3/ for high temperature plasmas, it has become necessary to consider the various cross sections for beam-plasma interactions which lead to beam attenuation and to excitation of the resonance line of atomic lithium. Knowledge of the relevant cross sections can serve as a guide in selecting the appropriate beam energy for a given measurement objective and plasma. This is particularly important for plasmas of large radius or high density where the attenuation can become quite significant if the beam energy is not optimized.

For the diagnostic purposes mentioned in /2,3/ we are interested in computing the intensity of the collisionally excited lithium resonance line as a function of beam position in the plasma. For beam interaction with a multi-component plasma, this intensity $N_{h\nu}$ in units of photons/cm^3-s -4π ster. is given by

$$N_{h\nu}(\ell) = n_e n_{Li}^o \exp\left[-\int_\ell n_e \sigma_T d\ell\right] \sum_j \frac{n_j}{n_e} {}_j\langle\sigma v\rangle^{exc} \quad +) \qquad (1)$$

where n_j is the number density of the j^{th} species, ${}_j\langle\sigma v\rangle^{exc}$ the corresponding excitation rate for the Li(2s-2p) line, n_e the electron density, n_{Li}^o the density of lithium atoms in the beam were there no plasma present, and the exponent takes into account the attenuation of the beam as it traverses the path ℓ through the plasma. Note that n_e, n_j, ${}_j\langle\sigma v\rangle^{exc}$ and σ_T

+) Formula (1) may also be written as

$$N_{h\nu}(\ell) = \frac{1}{e} J_b \, n_e \exp\left[-\int_\ell n_e \sigma_T dl\right] \sum_j \frac{n_j}{n_e} \frac{{}_j\langle\sigma v\rangle^{exc}}{v_b}$$

where J_b is the equivalent neutral beam current density $= n_{Li}^o v_b e$.

are all functions of position in the plasma. σ_T is the total cross section for beam attenuation by all plasma species,

$$\sigma_T = \frac{1}{n_e} \sum_{j,k} n_j \sigma_{j,k} \tag{2}$$

where $\sigma_{j,k}$ is the effective cross section for beam attenuation by the j^{th} species by the k^{th} process (either ionization, k= ; or charge-exchange k=cx) and

$$\sigma_{j,k} = {}_j\sigma^k_{eff} = \frac{{}_j\langle\sigma v\rangle^k}{v_b} , \tag{3}$$

v_b being the beam velocity. As an example, for the special case of a $Z_{eff} = 1$ plasma ($n_e = n_p$), σ_T takes the form

$$\sigma_T = \frac{1}{v_b}\left[{}_e\langle\sigma v\rangle^i + {}_p\langle\sigma v\rangle^i + {}_p\langle\sigma v\rangle^{cx}\right] = {}_e\sigma^i_{eff} + {}_p\sigma^i_{eff} + {}_p\sigma^{cx}_{eff} .$$

From Eqn.(1) we see that one may define an effective mean free path λ_{eff} for 1/e beam attenuation as

$$\lambda_{eff} = \frac{\ell}{\int_\ell n_e \sigma_T d\ell}$$

which becomes, for the case where σ_T is not a function of ℓ,

$$\lambda_{eff} = \frac{1}{\bar{n}_e \sigma_T}$$

$\bar{n}_e$ being the line-averaged density over the path ℓ.

Measured cross sections from the literature are available for the excitation of the Li(2s-2p) line by electrons, and for ionization of lithium atoms by electron impact and by charge exchange on protons. For ionization and Li(2s-2p) excitation by ions, a theoretical cross section must be used. In this case, the analytical expressions of Gryzinski have been employed. Because the Gryzinski formulations are simple and provide reasonable agreement with the known cross sections involving electron interactions, they are used in all calculations below with the exception of the charge exchange cross section. Here a fitted curve is utilized since the Gryzinski expression does not fit the experimental data.

First, the general formulas for computing the reaction rates of a monoenergetic beam with a Maxwellian plasma are summarized. The Gryzinski analytic forms are then described, followed by a comparison to the experimental data when it exists. Next, the calculated rate coefficients and effective cross sections are presented in graphical form along with a brief discussion of their principal features. Finally, some diagnostic possibilities suggested by examination of the various cross sections are listed.

All numerical calculations are carried out to an accuracy better than 0.5 %, which is far more precise than the Gryzinski theory or any of the experimental measurements.

2. General Formula for the Rate Coefficient

Referring to Fig.1 consider a monoenergetic beam of velocity $\vec{v}_b$ along the $\hat{v}_z$ axis interacting with target particles of mass m and velocity $\vec{v}$, the ensemble of which has a Maxwellian velocity distribution characterized by a temperature kT. The

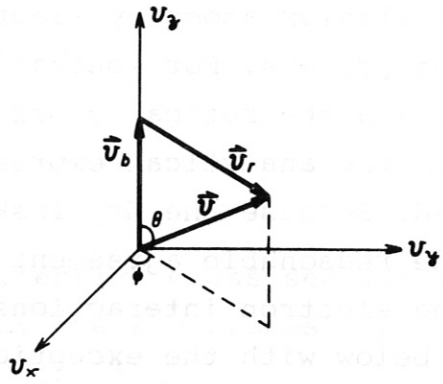

Fig. 1 Velocity Vector Diagram for the interaction of a monoenergetic beam of velocity $\vec{v}_b$ with a plasma particle of velocity $\vec{v}$.

rate coefficient $\langle \sigma v \rangle$ for a particular type of interaction with cross section $\sigma(v_r)$ is given by

$$\langle \sigma v \rangle = \int_0^\infty d^3v \; \sigma(v_r) \; v_r f(v) \tag{4}$$

where v_r is the relative velocity between the interacting plasma particle and the beam, and $f(v)d^3v$ is the plasma distribution function in velocity space. For a Maxwellian distribution

$$f(v) = \frac{1}{(\sqrt{\pi}\, w)^3} \; e^{-(v/w)^2} \qquad w^2 = \frac{2kT}{m} \; . \tag{5}$$

In spherical coordinates

$$d^3v = v^2 \, \text{Sine} \, d\theta \, d\phi \, dv,$$

and from the law of cosines

$$v_r = (v_b^2 + v^2 - 2v\, v_b \cos\theta)^{\frac{1}{2}}, \tag{6}$$

so that for a Maxwellian plasma

$$\langle \sigma v \rangle = \frac{1}{(\sqrt{\pi}\, w)^3} \int_0^{2\pi} d\phi \int_0^{\infty} dv\, v^2\, e^{-(v/w)^2} \int_0^{\pi} d\theta \sin\theta\, \sigma(v_r) v_r. \tag{7}$$

Because of cylindrical symmetry, the integration over ϕ may be carried out immediately. We then obtain

$$\langle \sigma v \rangle = \left(\frac{8kT}{\pi m}\right)^{\frac{1}{2}} \int_0^{\infty} d\chi\, \chi^2\, e^{-\chi^2} \int_0^{\pi} d\theta \sin\theta\, \sigma(\chi_r)\, \chi_r \tag{8}$$

where $\left(\frac{8kT}{\pi m}\right)^{\frac{1}{2}} = \bar{v}$ = average target paticle velocity

$$\chi = v/w$$

$$\chi_r = v_r/w = (\chi_b^2 + \chi^2 - 2\chi\chi_b \cos\theta)^{\frac{1}{2}}$$

$$\chi_b = v_b/w\ .$$

Equation (8) gives the reaction rate coefficient as used for calculations in this report. It remains to determine the cross section $\sigma(\chi_r)$ in terms of the normalized relative velocity χ_r.

3. Cross Sections

The principal advantage of the Gryzinski formulation is its ease of calculation combined with the surprisingly good agreement with experiment in many cases. In addition to Gryzinski's original work, comparisons between theory and experiment for electron and proton ionization are made by Freeman and Jones/4/, and for proton ionization by Garcia and Gerjuoy /5/. As illustrated in /4/, the agreement for electron interactions is generally excellent. Proton interactions are less accurately described, but for the lack of a better analytical theory or experimental measurements,the Gryzinski cross sections are employed here.Charge exchange cross sections are totally inadequately described by Gryzinski - see Garcia and Gerjuoy /6/ for comparisons between theory and experiment - and so the experimental data for protons charge exchanging on neutral lithium is used.

3.1 Gryzinski Cross Sections for Electrons

3.1.1 Ionization

According to Gryzinski the analytic form for single ionization, by an electron, of the i^{th} shell with ionization potential U_i for a target at rest, is

$$e\sigma_i^i = \frac{\sigma_o}{U_i^2} \, g_i(x) \qquad (9)$$

where

$$\sigma_o = 6.56 \times 10^{-14} eV^2 cm^2$$

$$g_i(x) = \frac{1}{x} \left(\frac{x-1}{x+1}\right)^{3/2} \left\{ 1 + \frac{2}{3}\left(1 - \frac{1}{2x}\right) \ln\left[2.7 + (x-1)^{\frac{1}{2}} \right] \right\}$$

$$x = E_e / U_i$$

E_e = kinetic energy of bombarding electron

U_i = binding energy of the orbital electron.

The total cross section is given by the summation of the cross sections for each shell. For lithium this assumes the form

$$ {}_e\sigma^i = \sum_{\ell=1}^{2} n_\ell \; {}_e\sigma_\ell^i \qquad (10) $$

where for the 1s electrons U_{1s}= 55 eV and n_ℓ = 2.
for the 2s electron U_{2s}= 5.39 eV and n_ℓ = 1.

The 1s shell potential is taken from Cauchois /7/. Single ionization of the 1s shell contributes about 1 % to ${}_e\sigma^i$ at E_e = 80 eV and about 12 % at E_e = 1 keV.

3.1.2 Li (2s-2p) Excitation

Taking into account the fact that the majority of transitions from the high energy levels of lithium pass through the 2p levels, the cross section for the 2s-2p transition is approximately equal to the cross section for the excitation of all levels of lithium. Using this approximation Gryzinski obtains

$$ {}_e\sigma^{exc} = Q\left(\frac{U_i}{U_{exc}} \; ; \; \frac{E_e}{U_{exc}}\right) - Q\left(1 \; ; \; \frac{E_e}{U_i}\right) \qquad (11) $$

where

$$ Q\left(\frac{U_i}{U_{exc}};\frac{E_e}{U_{exc}}\right) = \frac{\sigma_o}{U_{exc}^2} \; \frac{1}{x}\left(\frac{x}{1+x}\right)^{\frac{3}{2}} \left(1-\frac{y}{x}\right)^{1+\frac{1}{1+y}} \left\{ y + \frac{2}{3}\left(1-\frac{y}{2x}\right) \ln\left[2.7+(x-y)^{\frac{1}{2}}\right] \right\} $$

$$Q(1; \frac{E_e}{U_i}) = {}_e\sigma^i_{2s}$$

and $U_i = 5.39$ eV

U_{exc} = Excitation energy for the 2s-2p transition = 1.85 eV

$y = U_{exc}/U_i = 0.343$

The correction to ${}_e\sigma^{exc}$ due to the exchange process has not been included as it increases the cross section only slightly and then only at such low electron energies that the effect is of no importance for the plasmas considered in this report.

3.1.3 Experimental Measurements for Electrons and Comparison to Theory

From Fig.2 we see that there is excellent agreement between the Gryzinski ionization cross section and the experimental results of Aleksakhin et al /8/, Zapesochnyi et al /9/ and McFarland et al /10/. Jalin's /11/ data lies roughly a factor of two lower than the Gryzinski curve and the other experimental points and for this reason is not used to modify the Gryzinski curve.

Figure 3 illustrates the good agreement between the experimental results of Leep and Gallagher /12/, Hughes and Hendrickson /13/, Hafner and Kleinpoppen /14/ and the Gryzinski curve for Li (2s-2p) excitation. It should be noted that Hughes and Hendrickson, using a method proposed by Seaton /15/, put their measurements on an absolute basis by comparing the Li(2s-2p) curve to an absolutely determined Na(3s-3p) curve by Christoph /16/. The Hafner and Kleinpoppen measurements are also relative and have been normalized here to those of Hughes and Hendrickson. Leep and Gallagher obtained experimental results out to 1404 eV, their values being generally about 5 % larger

than those of Gryzinski in the range 100 - 1400 eV. The cross sections measured by Aleksakhin /8/ (Kiefer /17/) are substantially lower than the Gryzinski values. Nevertheless, if the slow fall-off with increasing energy is extrapolated to higher energies, which one must do in order to compute excitation rates, then one obtains cross sections larger than those predicted by Gryzinski. Altogether, this serves to demonstrate the caution with which such curves should be used with respect to the absolute values.

The fitted curve is of the form

$$ {}_e\sigma^i = 139 \times 10^{-16} \frac{E_e - 1.85}{E_e^{1.81}} \ln (0.81\, E_e)\ \mathrm{cm}^2. $$

3.2 Gryzinski Cross Sections for Ions

3.2.1 Ionization

The cross section for ionization of the i^{th} shell of a target at rest by a particle of mass m_i ($m_i \gg m_e$) and charge Z_i, with a bombarding energy E_i, is given by

$$ {}_i\sigma_i^i = \frac{\sigma_o'}{U_i^2} G\left(\frac{E_i}{U_i}\right) \qquad (12) $$

where

$$ \sigma_o' = 6.56 \times 10^{-14} Z_i^2\ \mathrm{eV}^2\ \mathrm{cm}^2 $$

$$G\left(\frac{E_i}{U_i}\right)=\frac{1}{x'}\left[\frac{x'}{1+x'}\right]^{\frac{3}{2}}\left\{\frac{x'}{1+x'}+\frac{2}{3}\left(1+\frac{1}{\alpha}\right)\ln\left[2.7+x'^{\frac{1}{2}}\right]\right\}\left[1-\frac{1}{\alpha}\right]\left[1-\left(\frac{1}{\alpha}\right)^{1+x'}\right]$$

$$x' = \frac{m_e}{m_i}\,\frac{E_i}{U_i}$$

$$\alpha = 4x'\left[1+\frac{1}{x'^{1/2}}\right].$$

This equation is valid above the apparent threshold $\alpha \geq 1$, which for the 2s electron yields upon solving for E_i,

$$E_i^{thr} = 78.2\ M_i U_i = 0.422\ M_i\ \text{keV}$$

where M_i is the weight of the bombarding particle in atomic mass units. As in the case of electrons, the total ionization cross section is obtained by summing the cross sections for the single ionization of each shell. For protons, single ionization of the 1s shell makes up about 1 % of ${}_p\sigma^i$ at E_p = 25 keV and about 10 % at E_p = 500 keV.

3.2.2 Li(2s-2p) Excitation

Once again, taking into account that the majority of transitions from the high energy levels of lithium pass through the 2p levels, the Gryzinski formula for excitation of the Li(2s-2p) line by ions becomes

$${}_i\sigma^{exc} = \frac{\sigma_o'}{U_{exc}^2}\,G\left(\frac{U_i}{U_{exc}};\ \frac{E_i}{U_{exc}}\right) - \frac{\sigma_o'}{U_i^2}\,G\left(1;\ \frac{E_i}{U_i}\right) \qquad (13)$$

where

$$G\left(\frac{U_i}{U_{exc}};\frac{E_i}{U_{exc}}\right)=\frac{1}{x'}\left[\frac{x'}{1+x'}\right]^{\frac{3}{2}}\left\{\frac{x'}{1+x'}\,y+\frac{2}{3}\left(1+\frac{y}{\alpha}\right)\ln\left[2.7+x'^{\frac{1}{2}}\right]\right\}\left[1-\frac{y}{\alpha}\right]$$

$$\cdot\left[1-\left(\frac{y}{\alpha}\right)^{1+x'}\right]$$

$$G(1; \frac{E_i}{U_i}) = {}_i\sigma^i_{2s}$$

and $U_i = 5.39$ eV.

The apparent threshold for excitation is given by $\alpha \geq y$, which yields

$$E_i^{thr} = 11.5\ U_i M_i = 0.062\ M_i \text{ keV}.$$

The correction to ${}_i\sigma^{exc}$ due to the capture process is not included in Eqn.(13) as it makes only a negligible difference in the case of a resonant line.

3.2.3 Discussion of Gryzinski Results for Ionization and Li(2s-2p) Excitation by Ions

The theoretical results for single ionization and Li(2s-2p) excitation by protons ($Z_i = 1$) are presented in Figs.4 and 5. For purposes of comparison the corresponding curves for electrons are also plotted. One sees, as is to be expected, that for high energies ($E_p > 10^5$ eV) the proton and electron cross sections are identical, when compared at the same velocity, so that in this energy range the proton cross sections are probably reasonably reliable. On the low energy side, which is where one would be in an experimental situation, the Gryzinski curves generally predict too large a cross section and the form is not always correct - see /4,5/ for comparisons for H,He,Ar,Ne and Kr.

None the less, even in the low energy range the curves are useful for predicting general trends and the rough order of magnitude of the cross sections.For example,referring to Figs.4 and 5 we see that with increasing energy the cross sections for

ionization and excitation can become quite appreciable. In particular, since σ_o' is proportional to Z_i^2, high Z ions will invariably begin to play a non-negligible role for relative velocities in the range of 10^8 cm/s.

3.3 Charge Exchange of Li^o on Protons

For charge exchange interactions, an analytic curve of the form ${}_p\sigma^{cx}(E_p) = 3 \times 10^{-15} E_p^2$ [keV] $e^{-.455 E_p}$ cm^2 has been fitted to the experimental points of Grüebler et al /18/ and Il'in et al (19). Should the cross section, in contrast, actually be non-zero at $E_p = 0$, then use of the analytic curve will lead to an underestimate of ${}_p\sigma^{cx}$ at low proton energies. We note also that Grüebler et al indicate an uncertainty of about $\pm$ 40 % in their measurements, and that the difference between /18/ and /19/ can be more than a factor of two, but not always in the same direction.

4. Rate Coefficients

4.1 Electrons

The expression for ${}_e\sigma^i$ Eqns.(9)-(10) [${}_e\sigma^{exc}$, Eqn.(11)] must be substituted into Eqn.(8) to compute the ionization (excitation) rate for electrons. For lithium beams and electron temperatures of practical interest in fusion-oriented plasmas, the relative velocity is determined to a very good approximation solely by the electrons i.e. $v_e \gg v_b$. Thus $v_r = v_e$, the integration over θ may be carried out immediately in Eqn.(8) and we obtain

$$\langle \sigma v \rangle = \bar{v} \int_{Z_{min}}^{\infty} dZ\, e^{-Z} Z\, \sigma(Z) \qquad (14)$$

where

$$z = \chi^2 = \frac{E_e}{T_e}$$

$$z_{min} = \frac{U_i}{T_e} \text{ for ionization, and } \frac{U_{exc}}{T_e} \text{ for excitation}$$

$\sigma(z)$ is derived by substituting $x = \frac{E_e}{U_i} = z\,\frac{T_e}{U_i}$ in Eqns.(9) and (11).

The rate coefficients $\langle \sigma v \rangle$ for ionization and excitation are plotted in Figures 7 and 18 respectively. In Fig.18 one sees that, in comparison to the Gryzinski curve, the fitted curve yields a substantially larger rate coefficient at high electron temperatures. This is due to the slower fall-off rate of the fitted curve with increasing energy and demonstrates the sensitivity of the rate coefficient to small changes in the form of the cross section at low energies.

4.2 Ions

4.2.1 Ionization and Li(2s-2p) Excitation

Since the ion and lithium masses are of the same order of magnitude, one cannot make the simplifying approximation $v_i \gg v_b$. Accordingly, the Gryzinski cross sections must be rewritten in terms of the relative velocity for use in Eqn.(8). From Eqn.(12) we have

$$x' = \frac{m_e}{m_i}\,\frac{E_i}{U_i} = \frac{m_e}{2U_i}\,v_i^2 \quad .$$

Replacing v_i with $v_r = \chi_r w_i$, x' becomes

$$x' = \frac{m_e}{2U_i}\,w_i^2\,\chi_r^2 = \frac{m_e}{m_i}\,\frac{T_i}{U_i}\,\chi_r^2 \qquad T_i[eV] = \frac{kT}{e} \quad ,$$

which may be directly substituted into the expressions for ionization, Eqn. (12), and excitation, Eqn. (13).

The rate coefficients for ionization and Li(2s-2p) excitation by H^+ and He^{2+} are shown in Figs. 8,9,19 and 20. The rate coefficients for other ions of charge Z_i and mass m_i may be taken from the proton curves by reading off at the equivalent proton temperature of $T_{eq} = T_i \frac{m_p}{m_i}$ and multiplying by Z_i^2. For example, for O^{8+} ions with a temperature of 800 eV we have $T_{eq} \sim (\frac{1}{16})\ 800 = 50$ eV, which at a beam energy of 8 keV gives $\langle \sigma v \rangle^i = 10^{-8} cm^3/s$. Finally, multiplying by $(8)^2$ we obtain 6.4×10^{-7} cm^3/s as the ionization rate for 800 eV O^{8+} ions on a 8 keV lithium beam.

For purposes of comparison and for use in the case of a low energy lithium beam where $v_i \gg v_b$ is a good approximation, the rates for ionization and excitation by electrons and protons for $v_b = 0$ are presented in Fig.17.

4.2.2 Charge Exchange of Li^o on Protons

The fitted curve for charge-exchange of protons on lithium is expressed in terms of the proton bombarding energy E_p. This may be converted to a relative energy E_r for use in Eqn.(8) by substituting v_r for v_p. Thus $E_p = \frac{1}{2} m_p v_p^2$ becomes

$$E_r = \tfrac{1}{2} m_p v_r^2 = \tfrac{1}{2} m_p (w_p \lambda_r)^2 = \tfrac{1}{2} m_p w_p^2 \lambda_r^2 = T_p[\text{eV}]\, \lambda_r^2 \ .$$

The exchange rate coefficient for the lithium beam energies 4-30 keV and 40-100 keV is given in Figures 10a and 10b respectively.

5. Effective Cross Sections and Comments

The effective cross sections, $\sigma_{eff} = \langle \sigma v \rangle / v_b$, for single ionization of lithium by electrons, protons, He^{2+} and for charge exchange of protons on lithium are shown in Figures 11,12,13 and 16 respectively. The following trends may be observed:

a) Ionization by Electrons

Because the ionization rate is independent of beam energy, increasing the beam energy always leads to a decrease in ${}_e\sigma^i_{eff}$. For very low beam energies, thermal for example, ${}_e\sigma^i_{eff}$ is so large ($\gg 10^{-14} cm^{-2}$) that significant beam penetration could be expected only for low density ($n_e \ll 10^{13} cm^{-3}$) plasmas, such as exist at the boundary of a Tokamak plasma.

b) Ionization and Li(2s-2p) Excitation by Ions

For $T_p < 1$ keV, the effective cross section for ionization by protons increases with increasing T_p and beam energy (${}_p\sigma^i_{eff} \lesssim 10^{-15} cm^2$). Above $T_p \simeq 1$ keV, increasing the beam energy leads to lower cross sections, but still ${}_p\sigma^i_{eff} \gtrsim 10^{-15} cm^2$.

For ions with $m_i \gg m_p$, ${}_i\sigma^i_{eff}$ increases with increasing E_b for the range ($T_i = 10$ eV - 10 keV) of ion temperatures indicated. Furthermore, as is demonstrated in Fig.14 for $E_b = 10$ keV, ${}_i\sigma^i_{eff}$ is essentially independent of the ion temperature for $T_i \lesssim 1$ keV. At higher beam energies this temperature independence will hold to even higher temperatures. Hence to a good approximation, ${}_i\sigma^i_{eff}$ may be taken directly from Fig.15 (Li beam bombarding target ions at rest) using the relationship

$$ {}_i\sigma^i_{eff} = {}_{Li}\sigma^i \; z_i^2 . $$

The same holds true for the excitation rate where

$$ {}_i\langle \sigma v \rangle^{exc} = {}_{Li}\langle \sigma v \rangle^{exc} \quad Z_i^2 , $$

and ${}_{Li}\langle \sigma v \rangle^{exc}$ is read from Fig.21. Because of the Z_i^2 dependence [Eqn.(12) and (13)], both ${}_i\sigma^i_{eff}$ and ${}_i\langle \sigma v \rangle^{exc}$ can become quite large for highly charged ions when the beam energy is high.

c) Charge Exchange on Protons

Below $T_p \simeq 700$ eV, the effective charge exchange cross section increases with increasing beam energy for $E_b \lesssim 30$ keV. Still higher beam energies lead to a decrease so that for $E_b \gtrsim 100$ keV, ${}_p\sigma^{cx}_{eff} \lesssim 10^{-15}\text{cm}^2$. For $T_p \gtrsim 700$ eV it is always advantageous to increase the beam energy. Note that for $E_b \gtrsim 100$ keV the effective cross section is largely independent of the proton temperature. In this case ${}_p\sigma^{cx}_{eff}$ may be directly read from Fig.6, where the conversion $E_b = (m_{Li}/m_p)E_p \backsim 7\ E_p$ must be made.

In summary, for low beam energies in conjunction with plasmas where $T_e \lesssim 1$ keV and $T_p \ll T_e$, beam attenuation will occur primarily due to ionization by electrons and charge exchange. As one increases the beam energy to the 30 keV region, the attenuation cross section also increases ($\sigma_T \backsim 8 \times 10^{-15}\text{cm}^2$!), charge exchange being by far the most important process. Still further increasing the beam energy leads to a decrease in ${}_p\sigma^{cx}_{eff}$ so that, at least theoretically, for $E_b \gtrsim 100$ keV the cross section for ionization by protons ($\max {}_p\sigma^i_{eff} \backsim 10^{-15}\ \text{cm}^2$) becomes larger than that for charge exchange and σ_T lies in the range $1 - 2 \times 10^{-15}\text{cm}^2$. For plasmas where $T_e \gtrsim 1$ keV and $T_p \lesssim T_e$, the situation is similar with the exception that an increase in beam energy always leads to a decrease in σ_T.

d) Impurity Ion Effects in More Detail

If $Z_{eff} \gg 1$, then attenuation due to ionization by and charge

exchange on impurity ions can become significant. Indeed, depending on the exact plasma composition and particle temperatures, it can happen that the above mentioned beneficial effects gained by increasing the beam energy are more than negated by the effects due to impurities. To quantify these statements somewhat we consider the expression for σ_T [Eqn.(12)] for the case of a single impurity species,

$$\sigma_T = {}_e\sigma^i_{eff} + \frac{n_p}{n_e}\left[{}_p\sigma^i_{eff} + {}_p\sigma^{cx}_{eff} \right] + \frac{n_i}{n_e}\left[{}_i\sigma^i_{eff} + {}_i\sigma^{cx}_{eff} \right]. \qquad (15)$$

We see that the presence of impurities leads to a "proton deficiency", i.e. $n_p < n_e$. That is to say, there are fewer protons on which charge exchange can occur, so that for plasmas and beam energies where proton charge exchange is otherwise the dominant beam attenuation process, the presence of impurities can lead to a smaller σ_T. The extent of this effect depends, among others, on Z_{eff} and Z_i. Using the relationships

$$Z_{eff} = \frac{1}{n_e}\sum_j n_j Z_j^2 = \frac{n_p}{n_e} + \frac{n_i Z_i^2}{n_e} \qquad (16a)$$

$$n_e = n_p + n_i Z_i \qquad (16b)$$

we find

$$\frac{n_p}{n_e} = \frac{Z_i - Z_{eff}}{Z_i - 1} \quad ,$$

from which it follows that for a given Z_{eff}, the "proton deficiency" is greatest for small values of Z_i, e.g. for light elements such as C^{6+} and O^{8+}. Thus, for the situation where ${}_i\sigma^i_{eff}$ and ${}_i\sigma^{cx}_{eff}$ are relatively unimportant, heavy impurities are more detrimental to beam penetration than are light ones.

At high beam energies ($E_b \sim 100$ keV) where the relative velocity is determined for both protons and impurities by the lithium beam velocity, we may write (see section 5b) ${}_i\sigma^i_{eff} = {}_{Li}\sigma^i Z_i^2$, so that

$$\frac{n_p}{n_e}\,{}_p\sigma^i_{eff} + \frac{n_i}{n_e}\,{}_i\sigma^i_{eff} = \left(\frac{n_p}{n_e} + \frac{n_i}{n_e}\,Z_i^2\right){}_{Li}\sigma^i = Z_{eff}\,{}_{Li}\sigma^i . \qquad (17)$$

The total cross section, Eqn.(15), becomes

$$\sigma_T = {}_e\sigma^i_{eff} + Z_{eff}\,{}_{Li}\sigma^i + \frac{n_p}{n_e}\,{}_p\sigma^{cx}_{eff} + \frac{n_i}{n_e}\,{}_i\sigma^{cx}_{eff} .$$

For $E_b \sim 100$ keV, using Figures 11, 15 and 16, ${}_e\sigma^i_{eff} < 10^{-15}\,cm^2$, ${}_{Li}\sigma^i \sim {}_p\sigma^{cx}_{eff} \sim 10^{-15}\,cm^2$. Therefore, when $Z_{eff} \gg 1$, even without considering charge exchange on impurities, σ_T is predicted to be quite large in spite of the high beam voltage.

With regard to the excitation rate at high beam energies, referring to Eqn. (1), and section 5b we may write

$$\frac{1}{n_e}\sum_j n_j \langle\sigma v\rangle^{exc} = {}_e\langle\sigma v\rangle^{exc} + \frac{1}{n_e}\sum_i n_i Z_i^2\,{}_{Li}\langle\sigma v\rangle^{exc} = {}_e\langle\sigma v\rangle^{exc} + Z_{eff}\,{}_{Li}\langle\sigma v\rangle^{exc} . \qquad (18)$$

Note that for lower beam energies where $v_b \gg v_p$ is no longer strictly valid, Eqn.(18) gives values for the total excitation rate which are too low. Examination of Fig.21 shows that already for $E_b = 20$ keV, ${}_{Li}\langle \sigma v \rangle^{exc} \simeq 4 \times 10^{-7}$ cm^3/s, which is comparable to the excitation rate due to electrons (Fig.18) for typical Tokamak plasma conditions. Hence if $Z_{eff} \gg 1$, then one would expect excitation to occur largely on impurities for $E_b \gtrsim 20$ keV. It should perhaps also be pointed out that for very large beam energies ${}_{Li}\langle \sigma v \rangle^{exc} \rightarrow 10^{-6}$ cm^3/s, so that if $Z_{eff} \gg 1$, the possibility exists that even for moderately dense plasmas ($n_e > 10^{13}$cm^{-3}) the 2s and 2p states will become equally populated, i.e. the lithium resonance line will go into saturation.

As a final comment with respect to the influence of impurities, it must be kept in mind that here the Gryzinski theory does not adequately describe the cross sections for ionization and excitation at low relative velocities. Cross section values near the peak ($E_b \lesssim 100 - 300$ keV) are probably accurate within a factor of two, but at lower energies these values can easily be in error by much more than a factor of two. Nevertheless, the general trends predicted are certainly accurate. Quantitatively, with respect to the charge exchange cross section for impurities, little can really be said. To date, there are no reliable theories which could furnish a basis for the calculation of such cross sections in the energy range of interest (say, $E_b < 300$ keV). In addition, the task of taking into account the multitude of charge states present in a plasma and the possibilities for charge-exchanging into the various excited states further complicates the problem.

Some Diagnostic Possibilities

In addition to the diagnostic application /2,3/ (Measurement of the current density profile in a Tokamak) for neutral lithium beams which motivated the calculations in this report,

examination of Eqn.(1) in conjunction with the various cross sections presented here suggests other diagnostic possibilities:

a) Measurement of Local Density Fluctuations

For the case where Li(2s-2p) excitation is due primarily to electrons, i.e. low beam voltages, Eqn.(1) may be written

$$N_{h\nu} = n_e n_{Li}^o \; {}_e\langle \sigma v \rangle^{exc} \; \exp\left[- \int_\ell n_e \sigma_T d\ell \right] . \qquad (19)$$

The Li(2s-2p) excitation rate (Fig.18) is a weak function of temperature; thus insofar as beam attenuation is unimportant $\left[\int_\ell n_e \sigma_T d\ell \ll 1\right]$, local fluctuations in n_e will be exactly mirrored as fluctuations in the photon emission rate $N_{h\nu}$, a quantity which can be easily measured. Such conditions would prevail, for example, for low-density laboratory plasmas ($n_e < 10^{12} cm^{-3}$) or at the border regions of a Tokamak plasma. Should $Z_{eff} \gg 1$, then measurement of $N_{h\nu}$ at high beam energies could yield information on impurity ion density fluctuations.

b) Measurement of the Density Profile

Again referring to Eqn.(19), for the case where ${}_e\langle \sigma v \rangle^{exc}$ is a weak function of position, i.e. where T_e does not vary strongly, and beam attenuation is negligible, measurement of $N_{h\nu}$ as a function of position will yield a profile proportional to n_e. The measurement becomes absolute to the extent that n_{Li}^o and ${}_e\langle \sigma v \rangle^{exc}$ are known, or if another method is available to calibrate the profile at one point. This effect could probably well be used in the boundary region of a Tokamak plasma where the above conditions hold and the density is so small that Thomson scattering becomes difficult.

c) Measurement of the Z_{eff} Profile

Referring to b), insofar as the excitation rate is determined largely by impurities at high beam energies, comparison of a $N_{h\nu}$ profile for high beam energies to a similar profile at low beam energies could yield information on the relative Z_{eff} profile [see Eqns.(1) and (18)]. An absolute measurement of Z_{eff} can be carried out only if ${}_e\langle\sigma v\rangle^{exc}$, ${}_{Li}\langle\sigma v\rangle^{exc}$ and n^o_{Li} are precisely known.

d) Measurement of the Plasma Line Density

The above diagnostics were based on observation of the lithium resonance line intensity as a function of position. Line-averaged information may also be gained by directly measuring the beam attenuation. Specifically, examination of Eqn.(1) shows that the beam attenuation n_{Li}/n^o_{Li} over a path ℓ is given by

$$\frac{n_{Li}}{n^o_{Li}} = e^{-\int n_e \sigma_T d\ell}.$$

One sees immediately that, for the special case where σ_T is known and is independent of position, the line-averaged electron density may be calculated from

$$\bar{n}_e = \frac{1}{\ell}\int_o^{\ell} n_e d\ell = \frac{1}{\ell\,\sigma_T}\ln\left(\frac{n^o_{Li}}{n_{Li}}\right).$$

The accuracy with which $\bar{n}_e$ may be determined depends largely on the precision to which σ_T is known, which in turn depends on the reliability of the relevant cross sections presented in this report. Should $Z_{eff} > 1$, then matters become more complicated if not impossible since the cross sections for

charge exchange on impurities are not known. More detailed examples of diagnostic capabilities, which may be extended to lithium beams, using beam attenuation are to be found in /20,21/ for hydrogen beams and in /22/ for a potassium beam.

Acknowledgement

I would like to thank Miss H. Sittig for drawing the many Figures contained in this report.

References

/1/ M.Gryzinski, Phys.Rev. 138, A 336 (1965)

/2/ J.Fujita and K.McCormick, 6th Eur.Conf.on Contr.Fusion and Plasma Phys., Moscow, 141 (1973)

/3/ K.McCormick, M.Kick and J.Olivain, 8th Eur.Conf.on Contr. Fusion and Plasma Phys., Prague, 40, (1977)

/4/ R.L.Freeman and E.M.Jones,Culham Lab.Report CLM-R 137 (1974)

/5/ J.D.Garcia, E.Gerjuoy and J.E.Welker, Phys.Rev.165, 66 (1968)

/6/ J.D.Garcia, E.Gerjuoy and J.E.Welker, Phys.Rev.165, 165 (1968)

/7/ Y.Cauchois, J.Phys.Radium 16, 262 (1955)

/8/ I.S.Aleksakhin, I.P.Zapesochny and O.B.Shpenik, 5th Int. Conf.Phys.Elec. and At. Collisions, Leningrad, 1967,p.499

/9/ I.P.Zapesochnyi and I.S.Aleksakhin, Soviet Physics JETP 28, 41 (1969)

/10/ R.H.McFarland and J.D.Kinney, Phys.Rev.137, A 1058 (1965)

/11/ R.Jalin, R.Hagemann and R.Botter, J.Chem.Phys.59, 952 (1973)

/12/ D.Leep and A.Gallagher, Phys.Rev.A 10, 1082 (1974)

/13/ R.H.Hughes and C.G.Hendrickson,J.Opt.Soc.Am.54, 1494 (1964)

/14/ Hafner and Kleinpoppen,from a Review by B.I.Moiseiwitsch and S.J.Smith, Rev.Mod.Phys.40, 310 (1968)

/15/ M.J.Seaton, Atomic and Molecular Processes, edited by D.R.Bates (Academic Press Inc., New York, 1962),p.374

/16/ W.Christoph, Ann.Phys. (Leipzig) 23, 51 (1935)

/17/ L.J.Kieffer, Atomic Data 1, 132 (1969)

/18/ W.Grüebler, P.A.Schmelzbach, V.König and P.Marmier, Helvetica Physica Acta 43, 254 (1970)

/19/ R.N.Il'in, Y.A.Oparin, E.S.Solov'ev and N.V.Fedorenko, Soviet Physics - Technical Physics 11, 924 (1967)

/20/ Y.V.Afrosimov, B.A.Ivanov, A.I.Kislyakov and M.P.Petrov, Soviet Physics - Technical Physics 11, 63 (1966)

/21/ A.I.Kislyakov and M.P.Petrov, Soviet Physics - Technial Physics 15, 1252 (1971)

/22/ V.A.Finlayson, F.H.Coensgen and W.E.Nexsen,Jr., Nuclear Fusion 12, 659 (1972)

Figure Captions

Fig. 1: Velocity Vector Diagram for the interaction of a monoenergetic beam of velocity $\vec{v}_b$ with a plasma particle of velocity $\vec{v}$.

Fig. 2: Experimental and Gryzinski cross sections for the ionization of lithium by electrons.

Fig. 3: Experimental and Gryzinski cross sections for Li(2s-2p) excitation by electrons.

Fig. 4: Gryzinski cross section for the ionization of lithium by protons.

Fig. 5: Gryzinski cross section for Li(2s-2p) excitation by protons.

Fig. 6: Experimental cross sections for the charge exchange of protons on lithium as a function of proton energy.

Fig. 7: Rate coefficient for the ionization of lithium by electrons.

Fig. 8: Rate coefficient for the ionization of lithium by protons with lithium beam energy as a parameter.

Fig. 9: Rate coefficient for the ionization of lithium by He^{2+} with lithium beam energy as a parameter.

Fig.10: Rate coefficient for the charge exchange of protons on lithium

a) Lithium beam energies 4 - 30 keV

b) Beam energies 40 - 100 keV

Fig.11: Effective cross section for ionization of lithium by electrons.

Fig.12: Effective cross section for ionization of lithium by protons with lithium beam energy as a parameter

Fig.13: Effective cross section for ionization of lithium by He^{2+} with lithium beam energy as a parameter.

Fig.14: Effective cross section for ionization of lithium by C^{6+}, O^{8+}, Fe^{20+} and Mo^{32+} for a 10 keV lithium beam.

Fig.15: Gryzinski cross section for the ionization of lithium by protons as a function of lithium beam energy.

Fig.16: Effective cross section for charge exchange of protons on lithium
a) Lithium beam energies 4 - 30 keV
b) Beam energies 40 - 100 keV

Fig.17: Rate coefficients for Li(2s-2p) excitation and ionization of lithium by electrons and protons for $v_b = 0$.

Fig.18: Li(2s-2p) excitation rate for electrons.

Fig.19: Li(2s-2p) excitation rate for protons with lithium beam energy as a parameter.

Fig.20: Li(2s-2p) excitation rate for He^{2+} with lithium beam energy as a parameter.

Fig.21: Li(2s-2p) excitation rate for protons as a function of lithium beam energy.

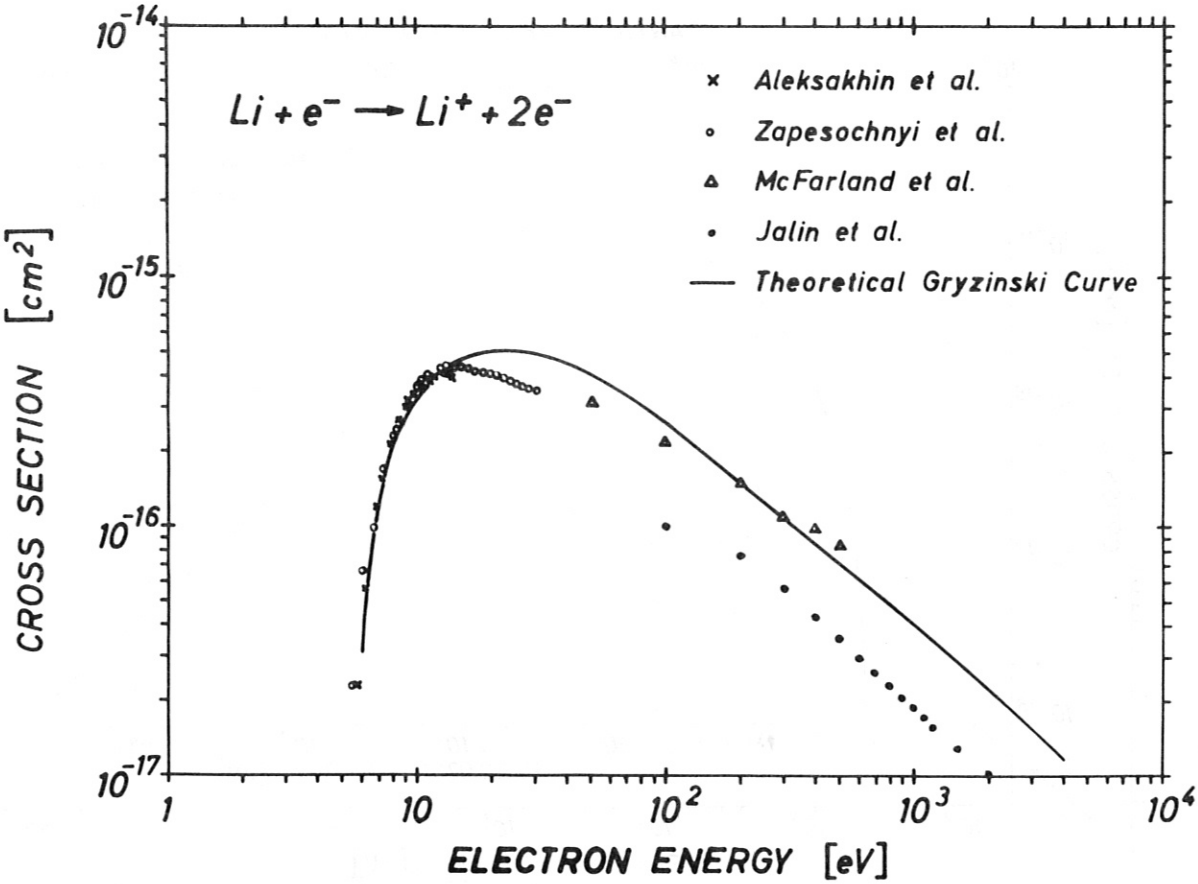

Fig. 2 Cross sections for the ionization of lithium by electrons.

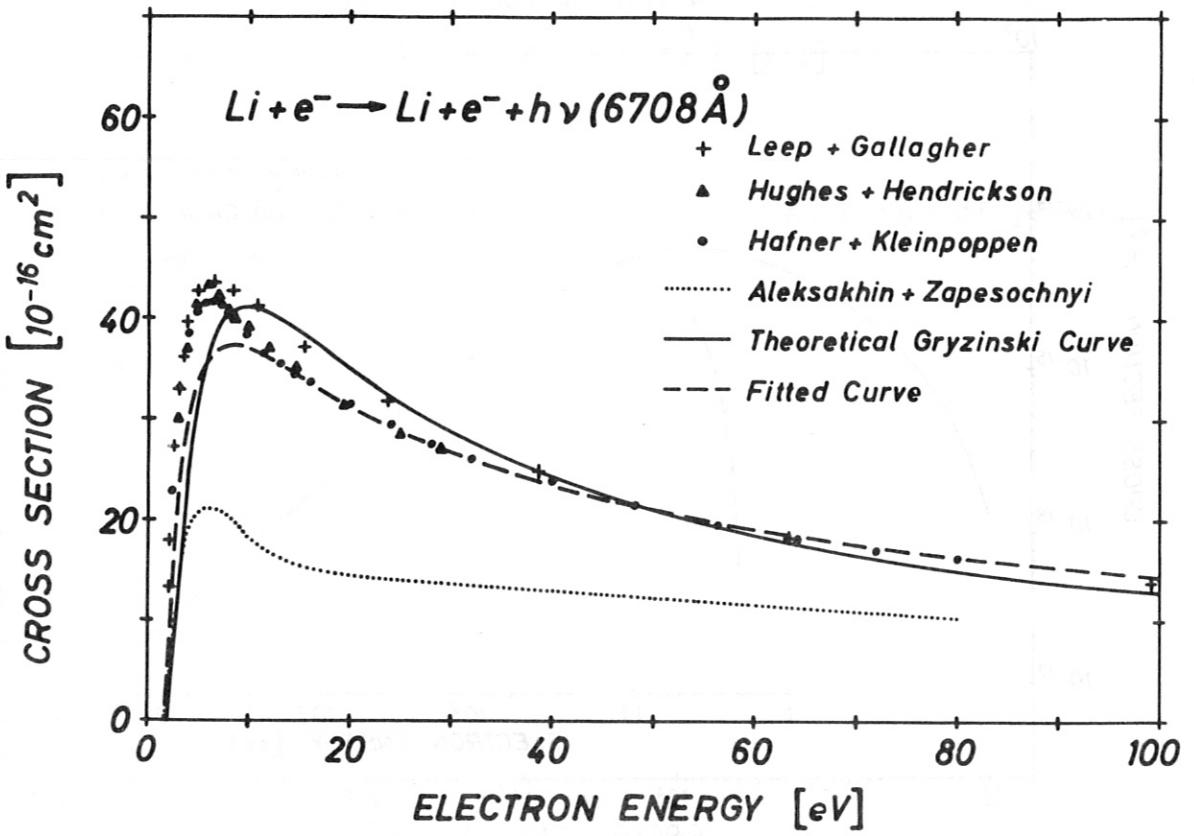

Fig. 3 Cross sections for Li(2s-2p) excitation by electrons.

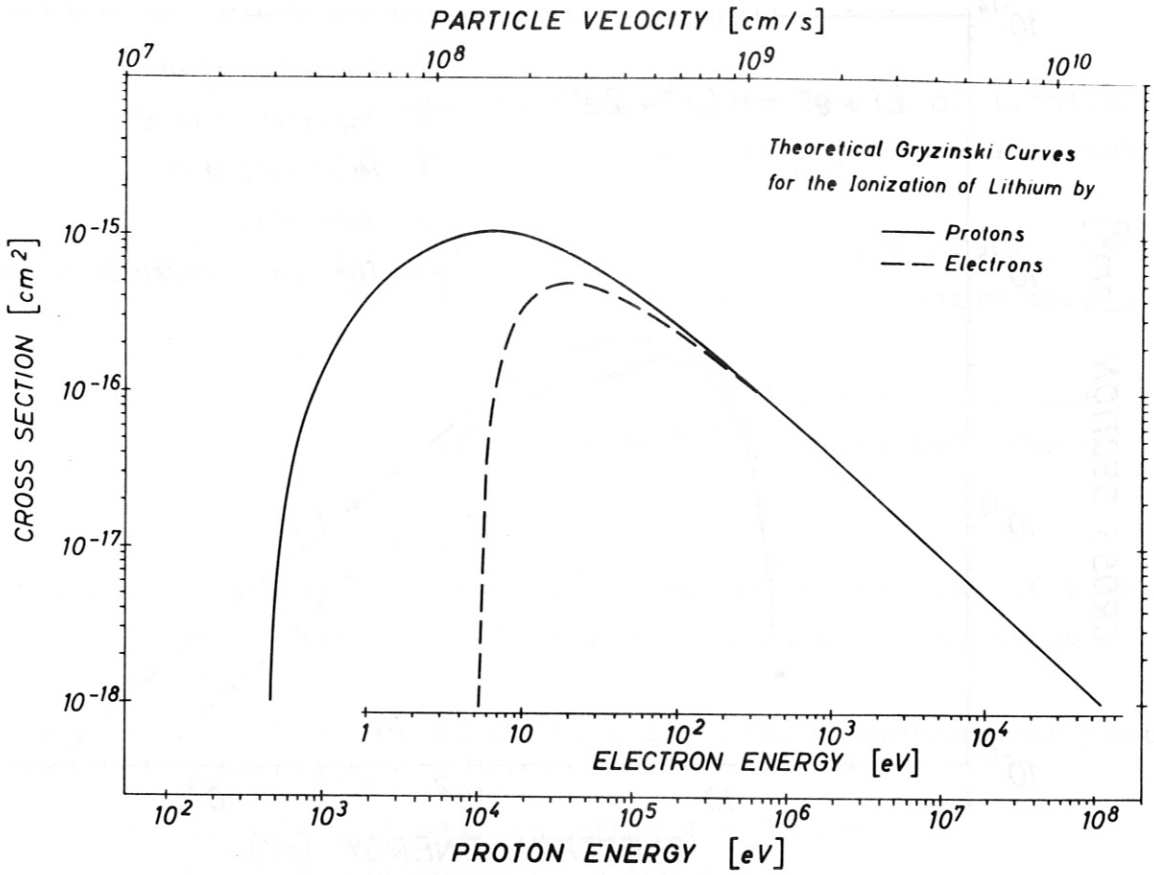

Fig. 4 Gryzinski cross section for the ionization of lithium by protons.

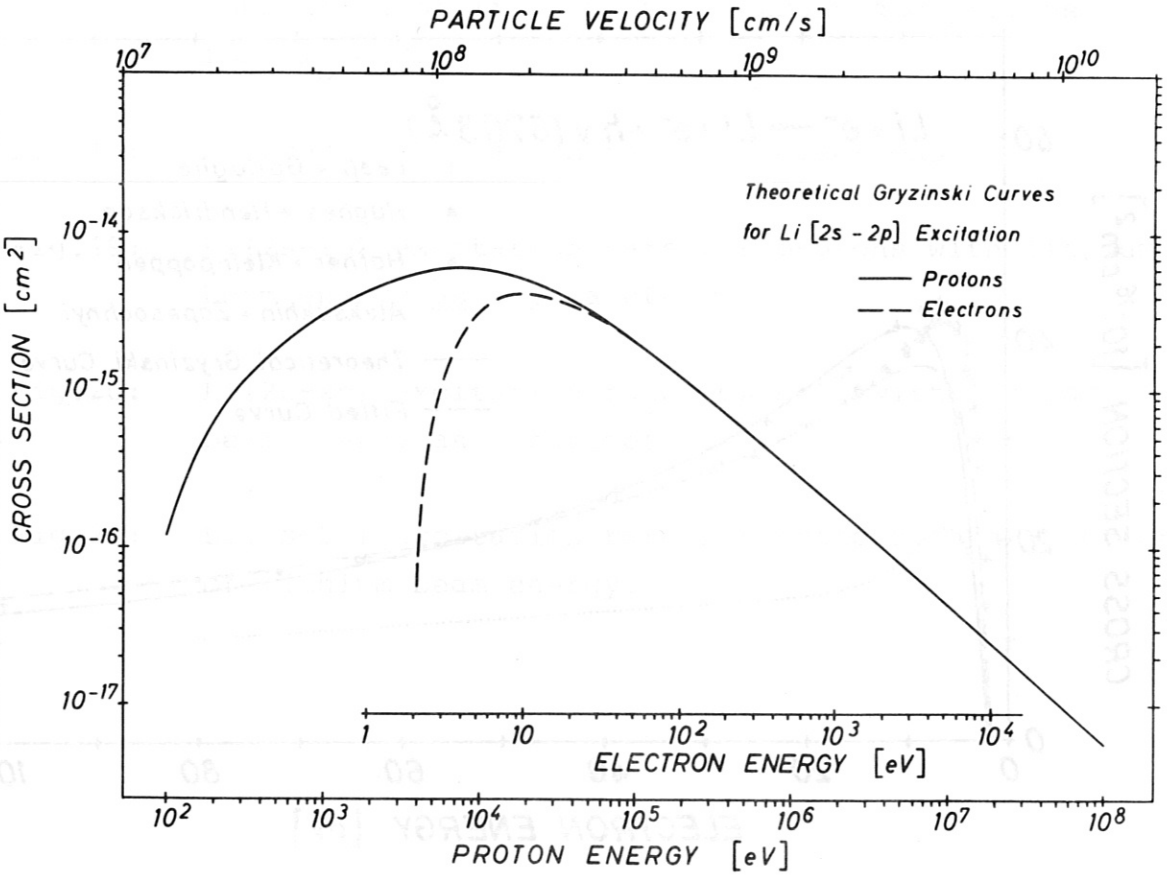

Fig. 5 Gryzinski cross section for Li(2s-2p) excitation by protons.

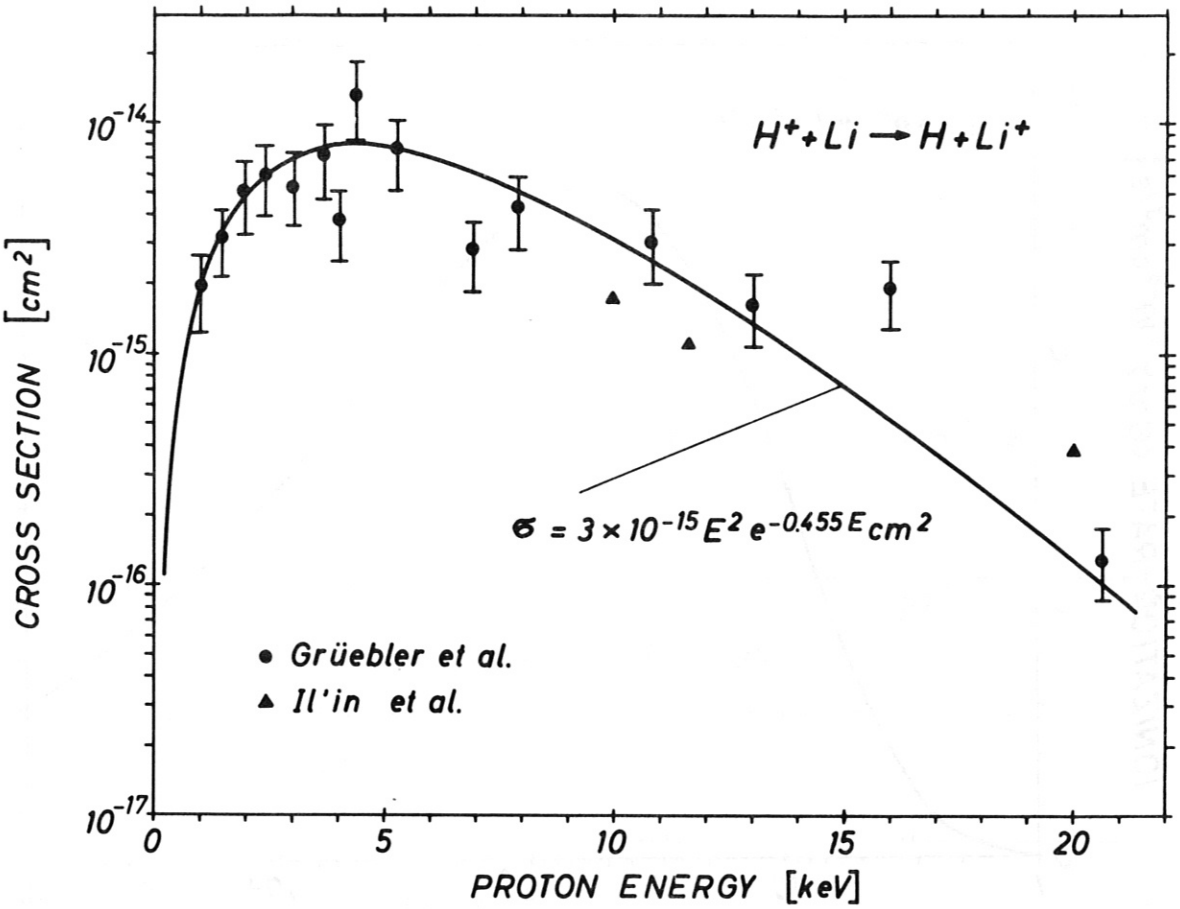

Fig. 6 Cross sections for the charge exchange of protons on lithium.

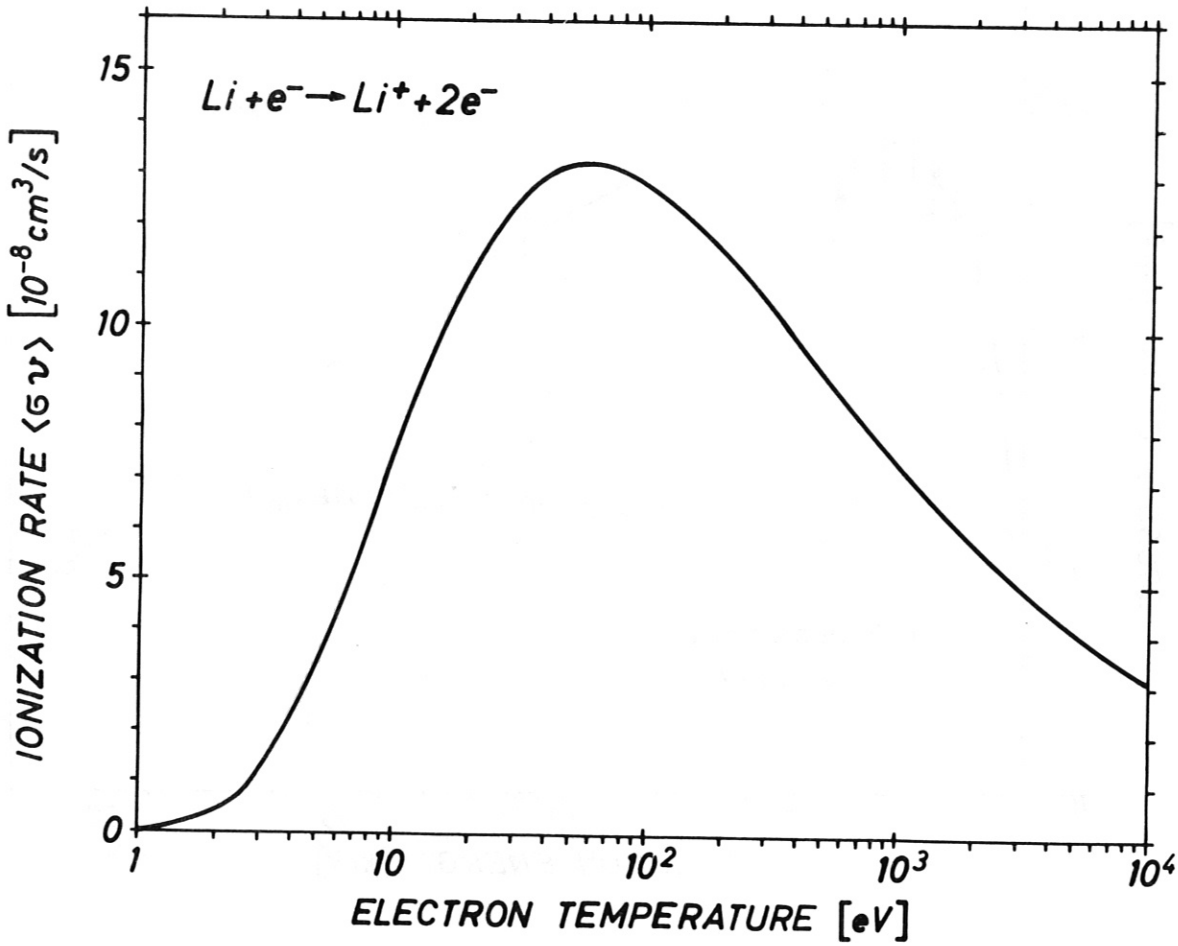

Fig. 7 Rate coefficient for the ionization of lithium by electrons.

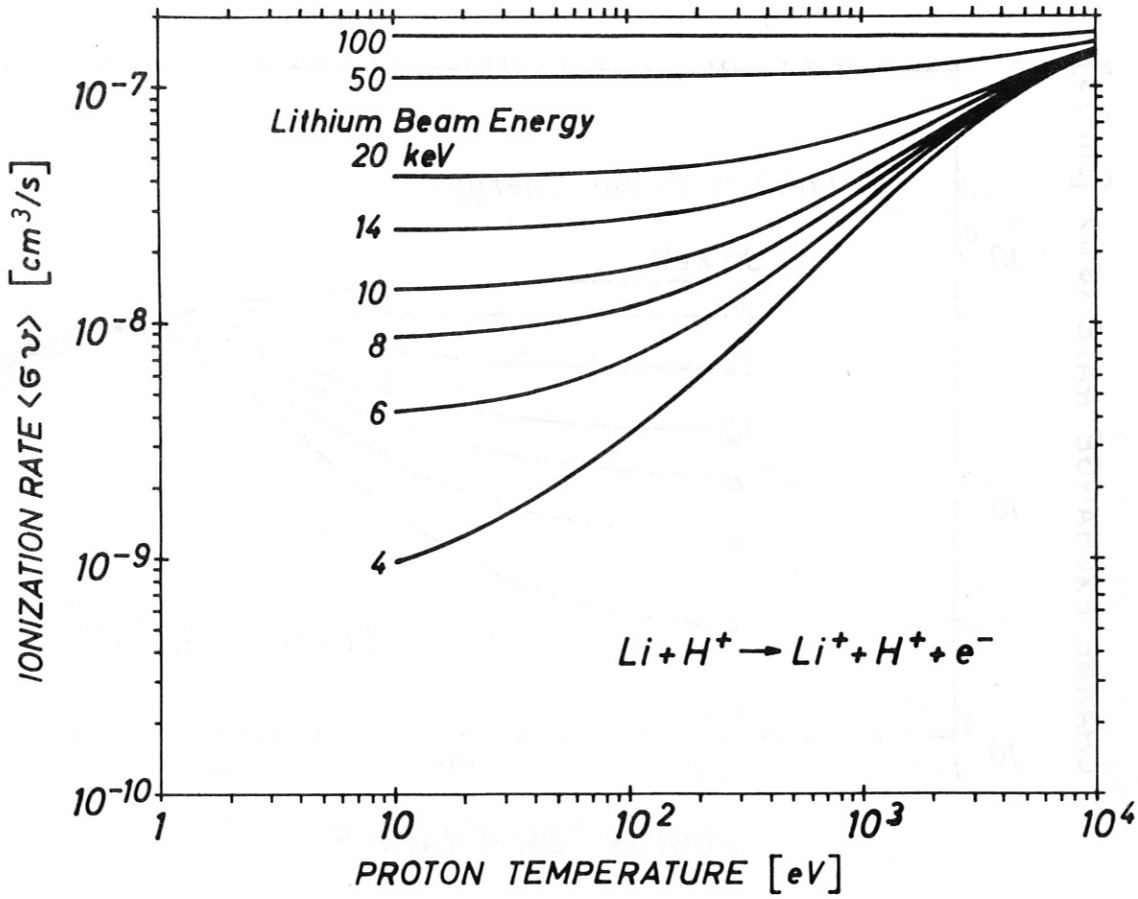

Fig. 8 Rate coefficient for the ionization of lithium by protons.

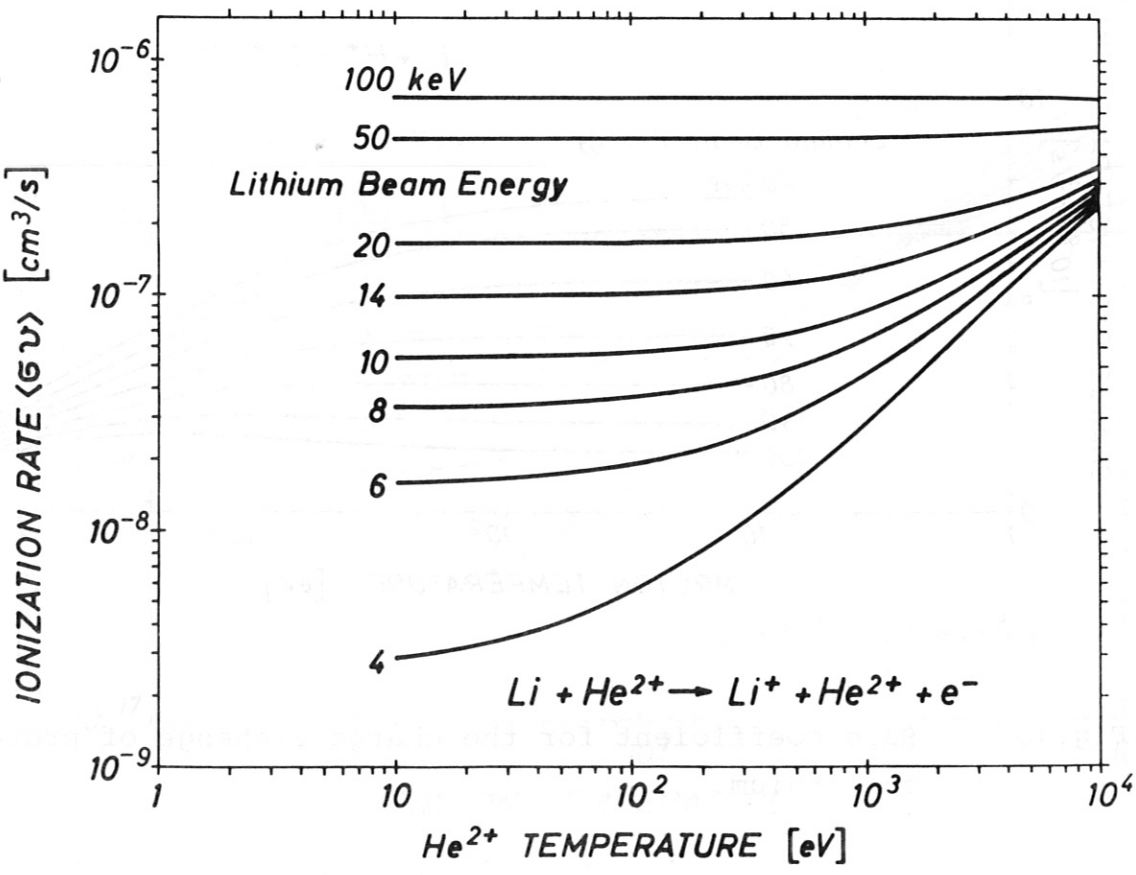

Fig. 9 Rate coefficient for the ionization of lithium by He^{2+}.

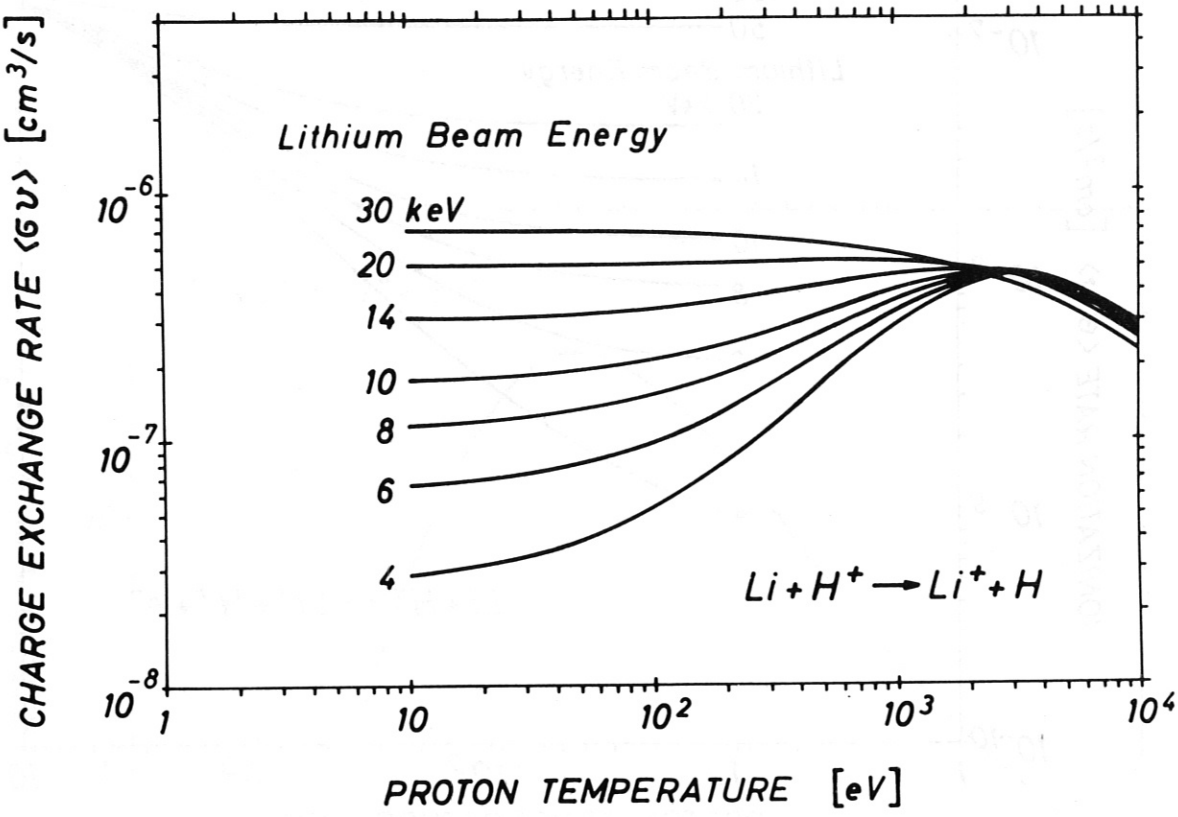

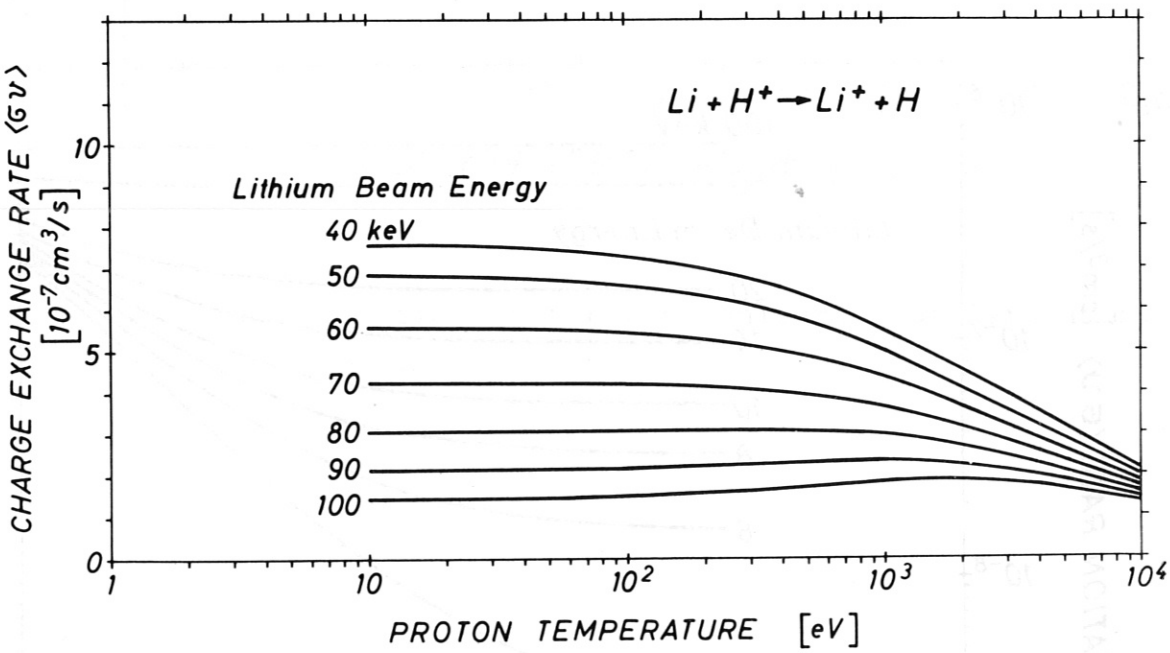

Fig.10 Rate coefficient for the charge exchange of protons on lithium.

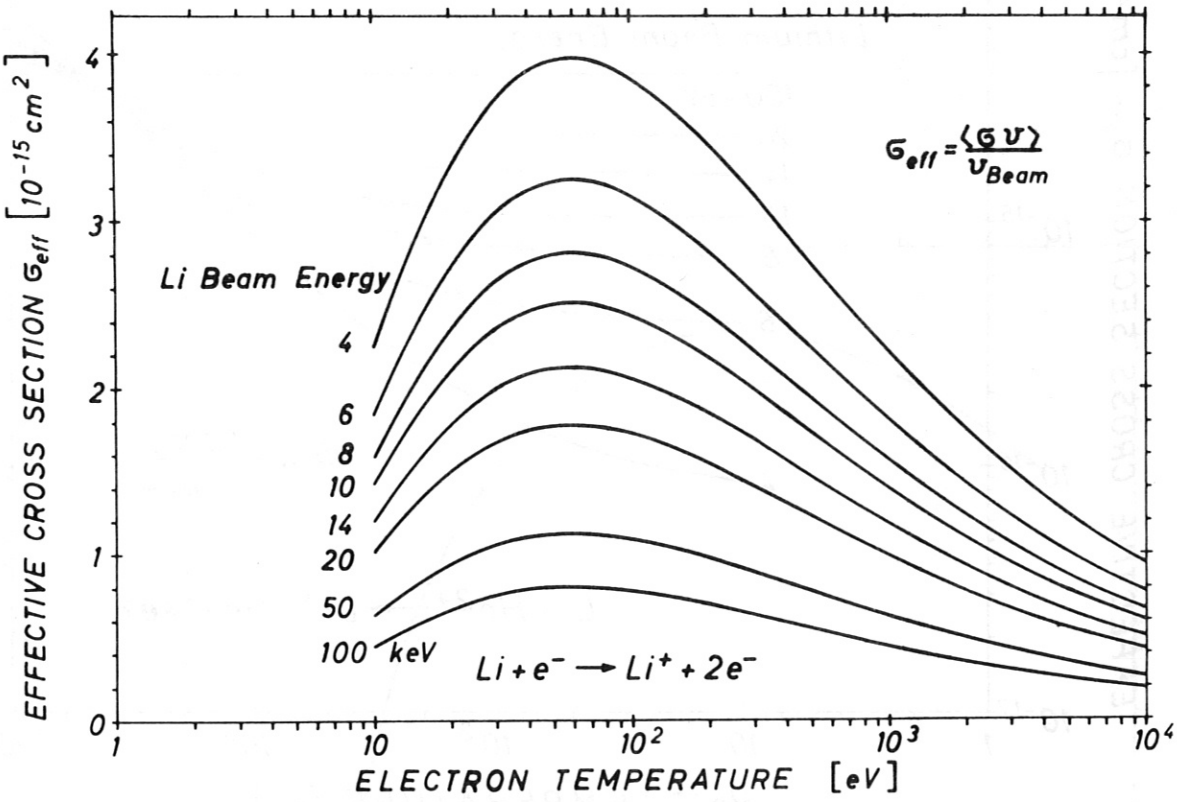

Fig.11 Effective cross section for the ionization of lithium by electrons.

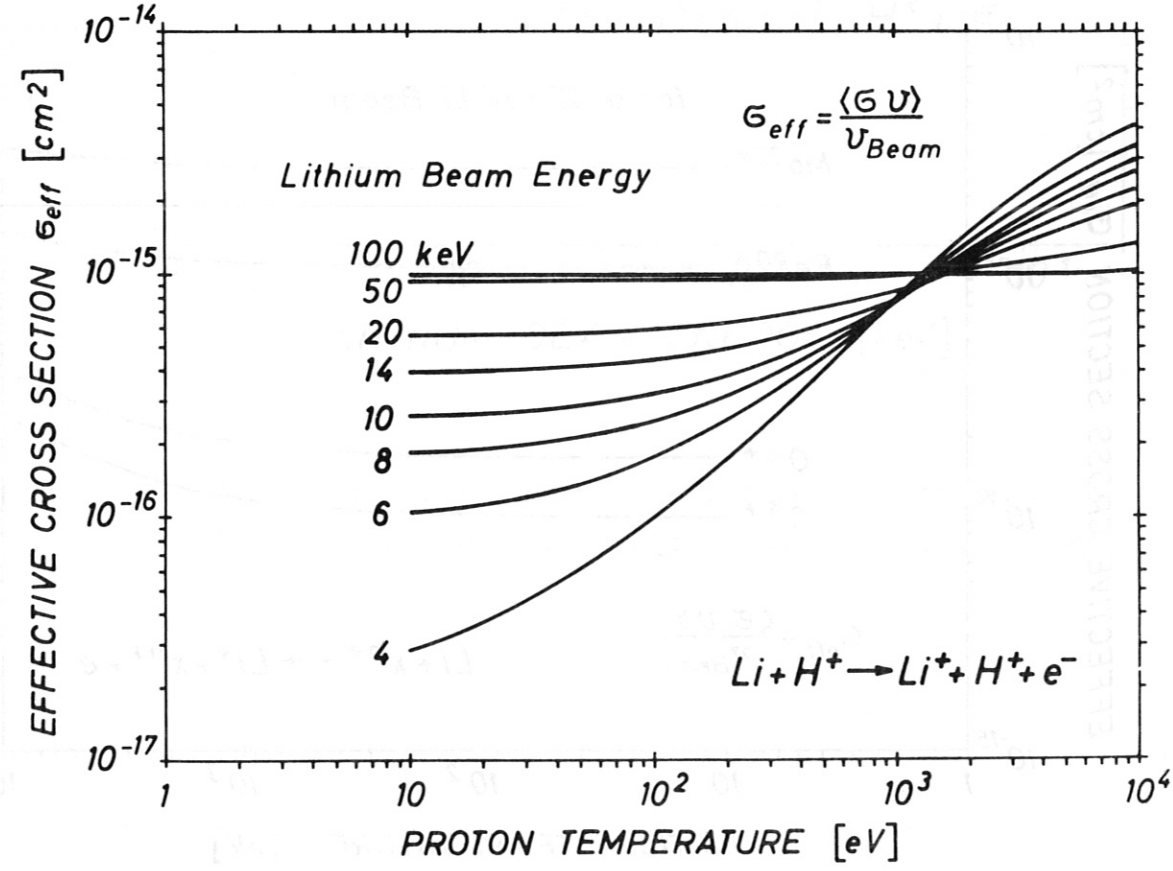

Fig.12 Effective cross section for the ionization of lithium by protons.

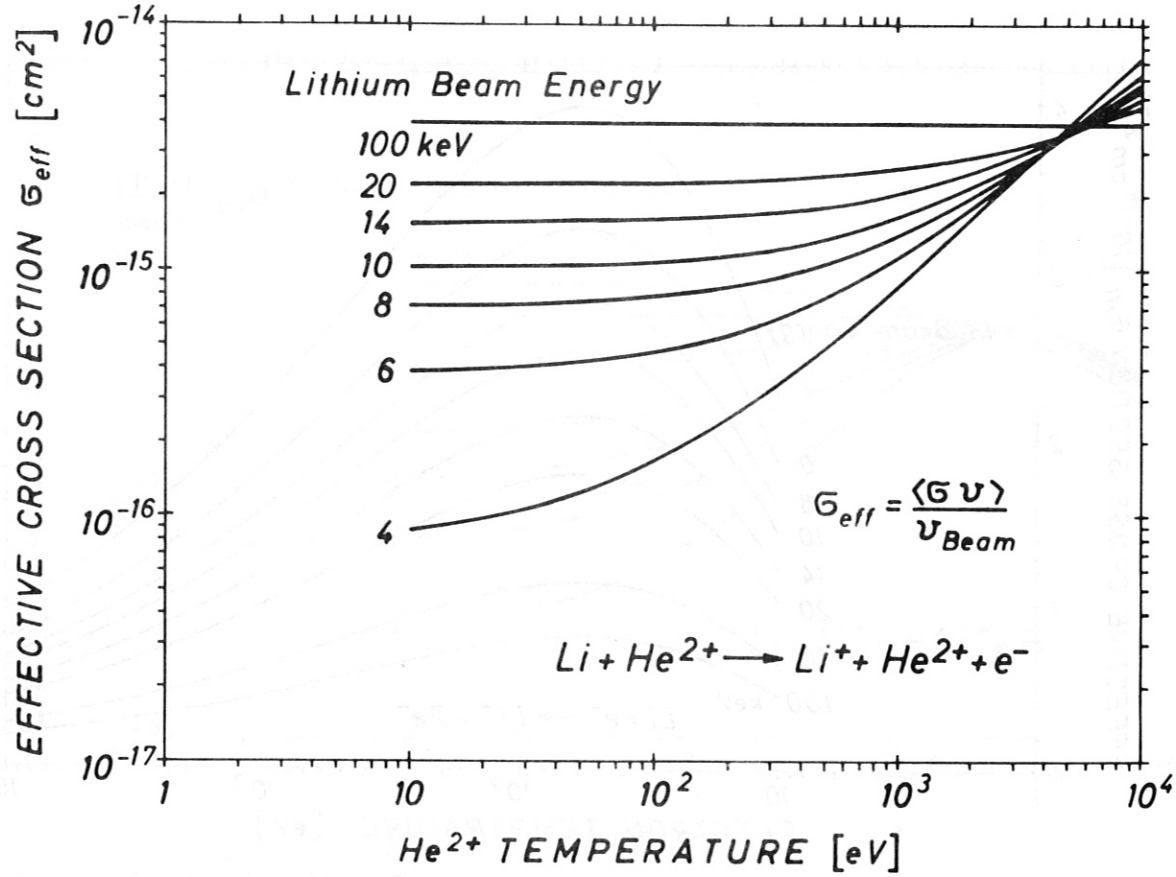

Fig.13 Effective cross section for the ionization of lithium by He^{2+}.

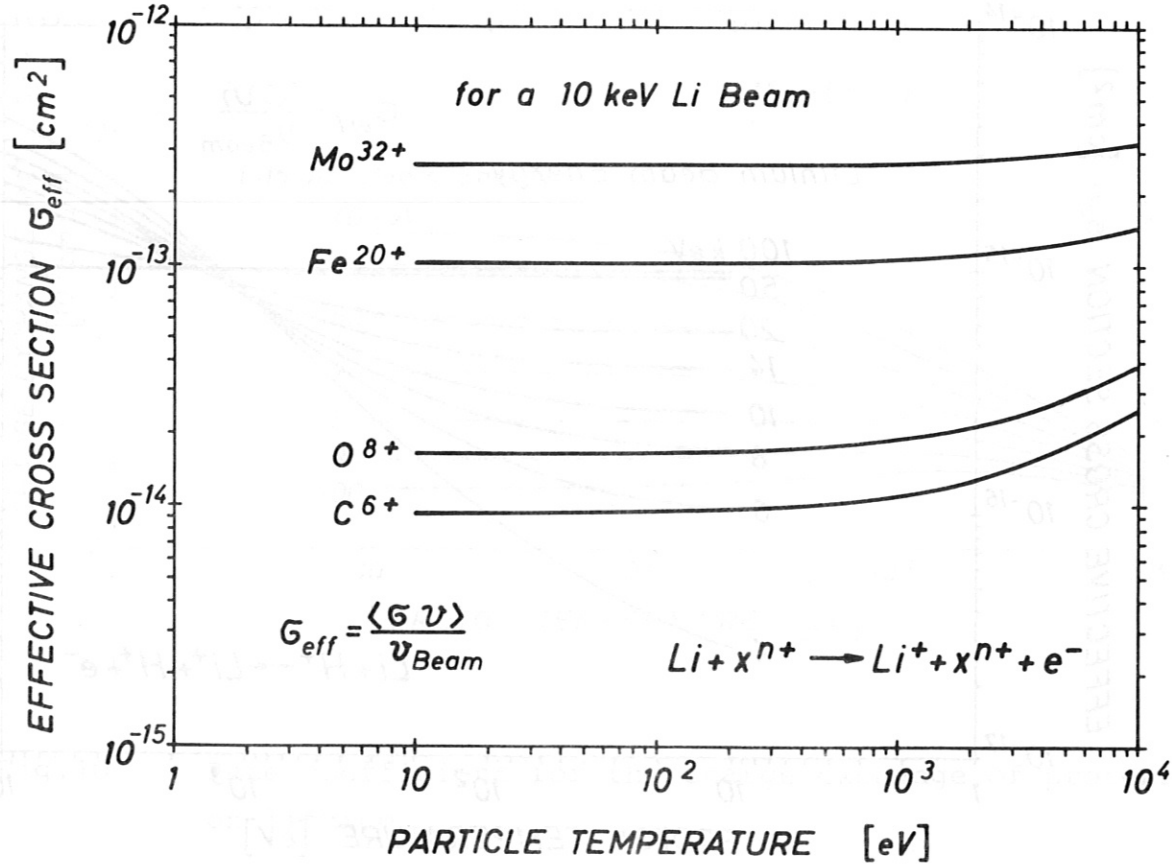

Fig.14 Effective cross section for the ionization of lithium by C^{6+}, O^{8+}, Fe^{20+} and Mo^{32+} for a 10 keV lithium beam.

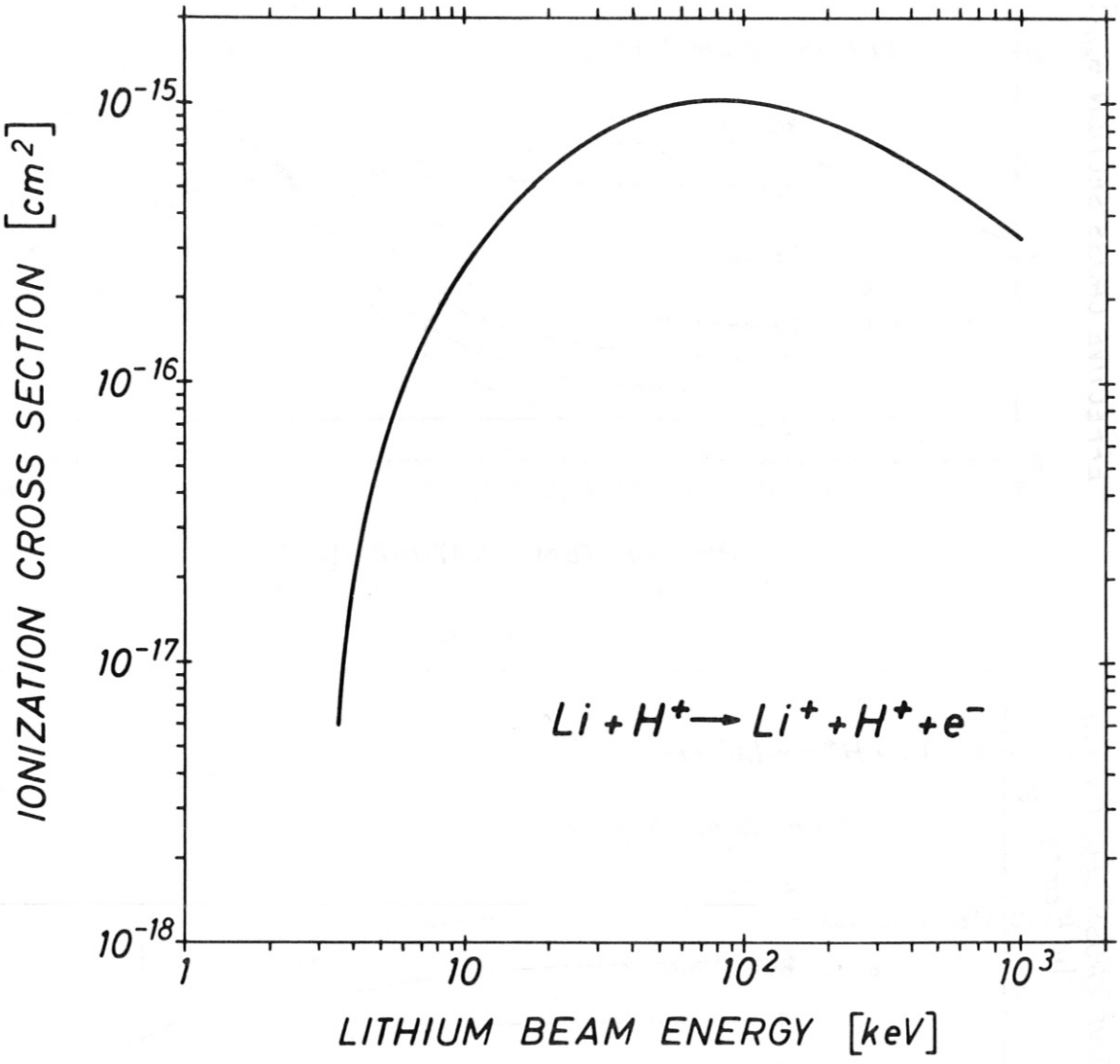

Fig.15 Gryzinski cross section for the ionization of lithium by protons as a function of lithium beam energy.

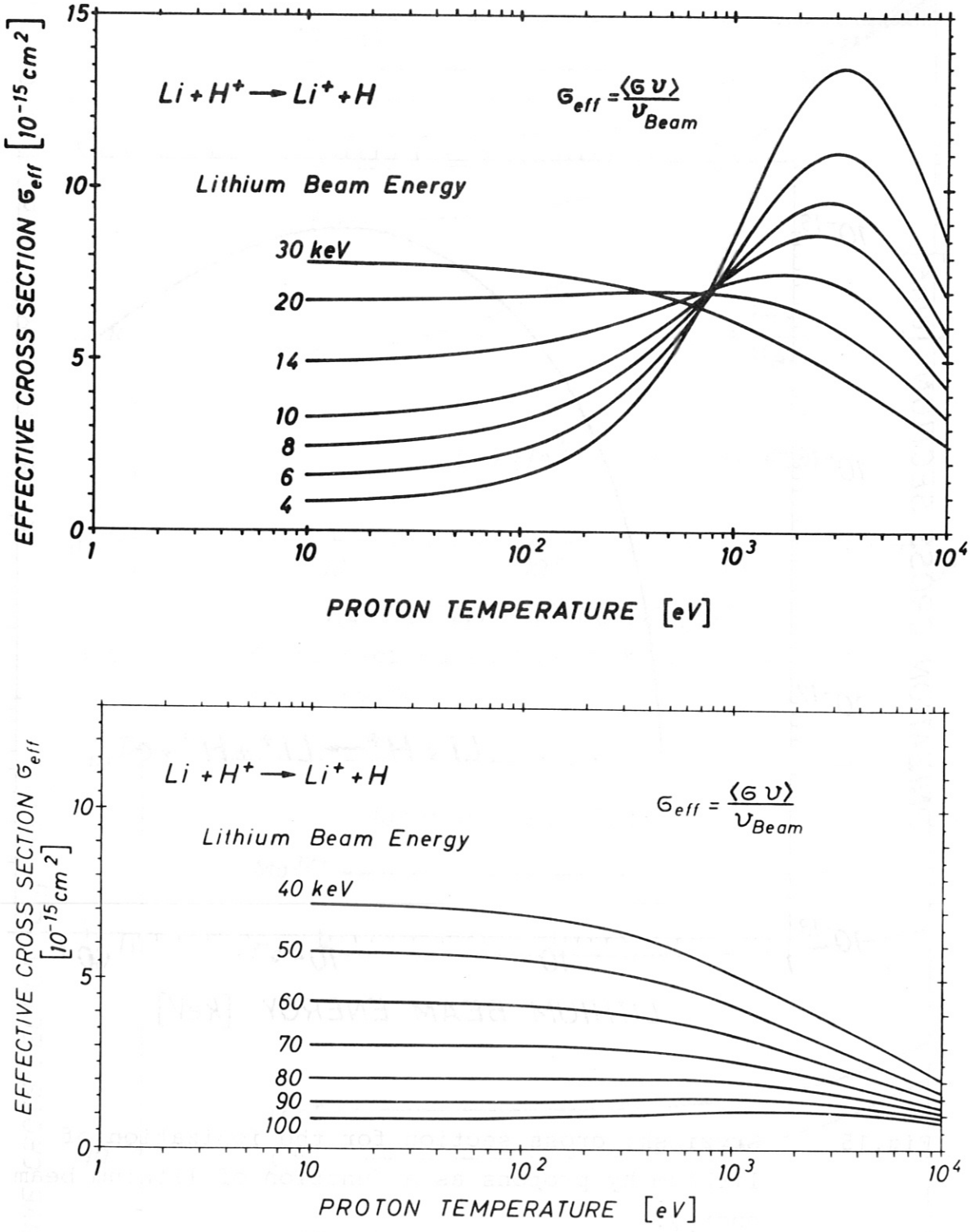

Fig.16 Effective cross section for the charge exchange of protons on lithium.

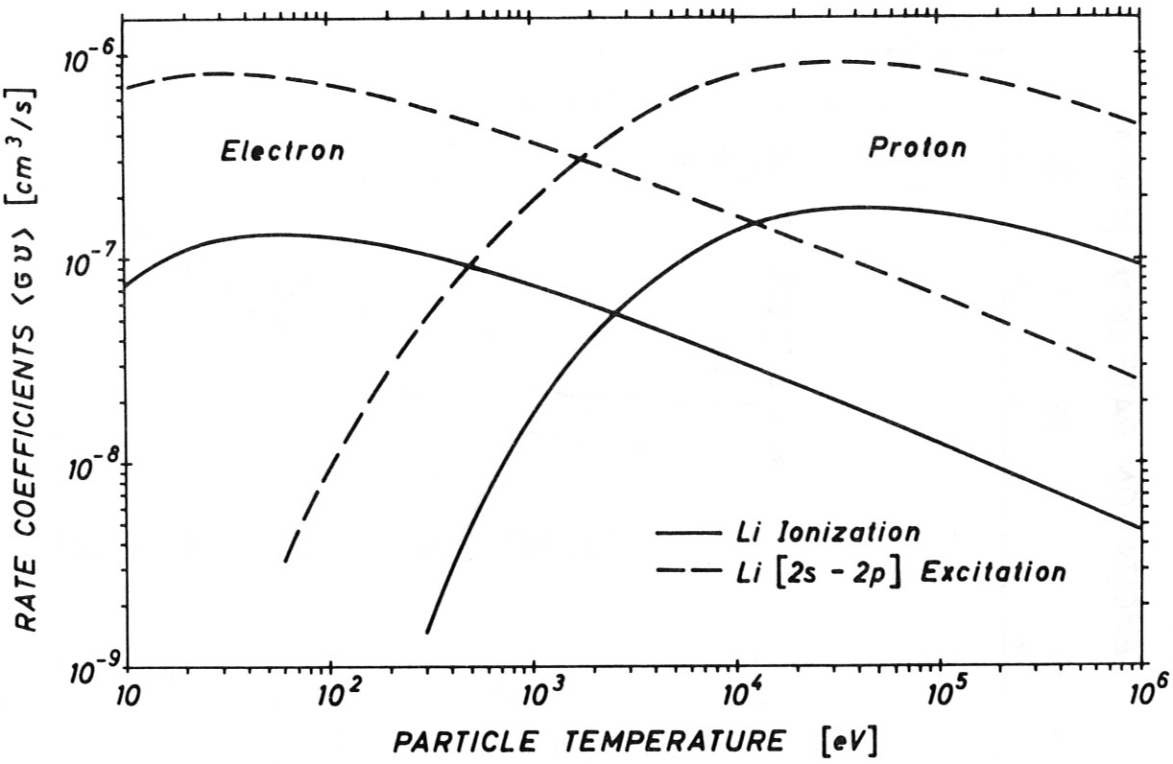

Fig.17 Rate coefficients for Li(2s-2p) excitation and ionization of lithium by electrons and protons for zero beam velocity.

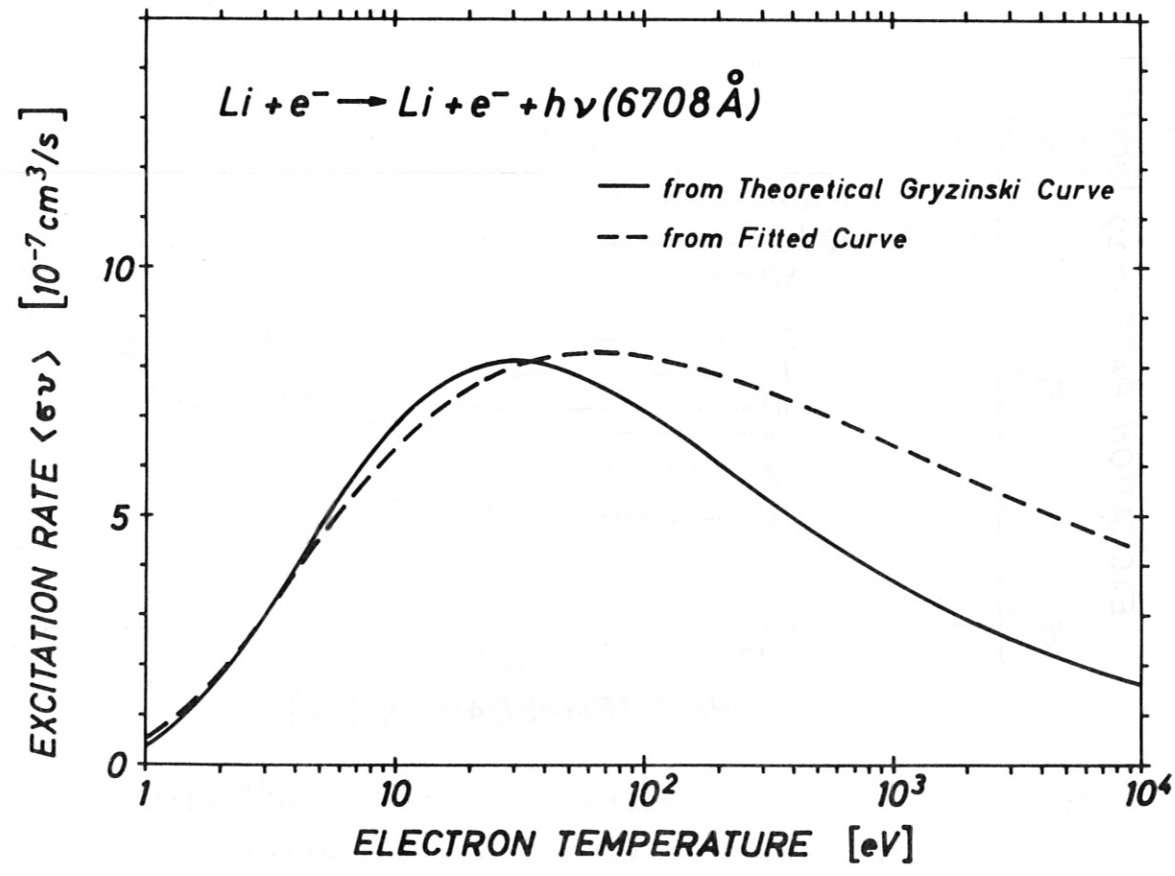

Fig.18 Li(2s-2p) excitation rate for electrons.

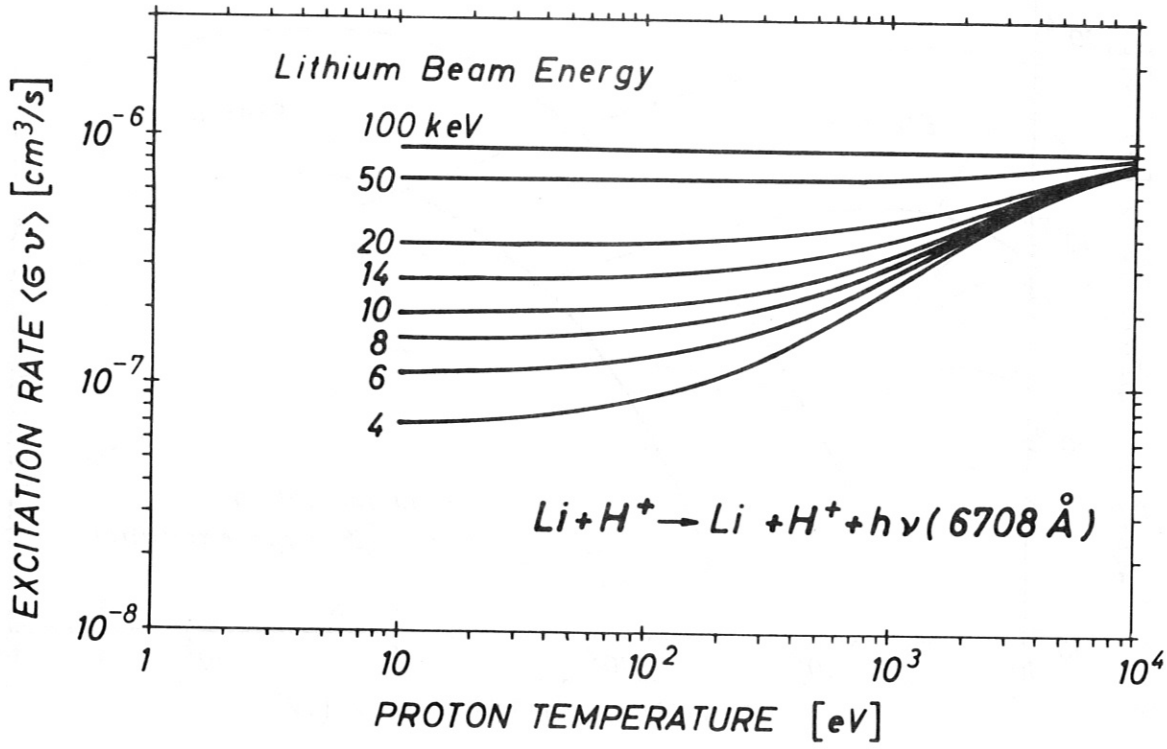

Fig.19 Li(2s-2p) excitation rate for protons with lithium beam energy as a parameter.

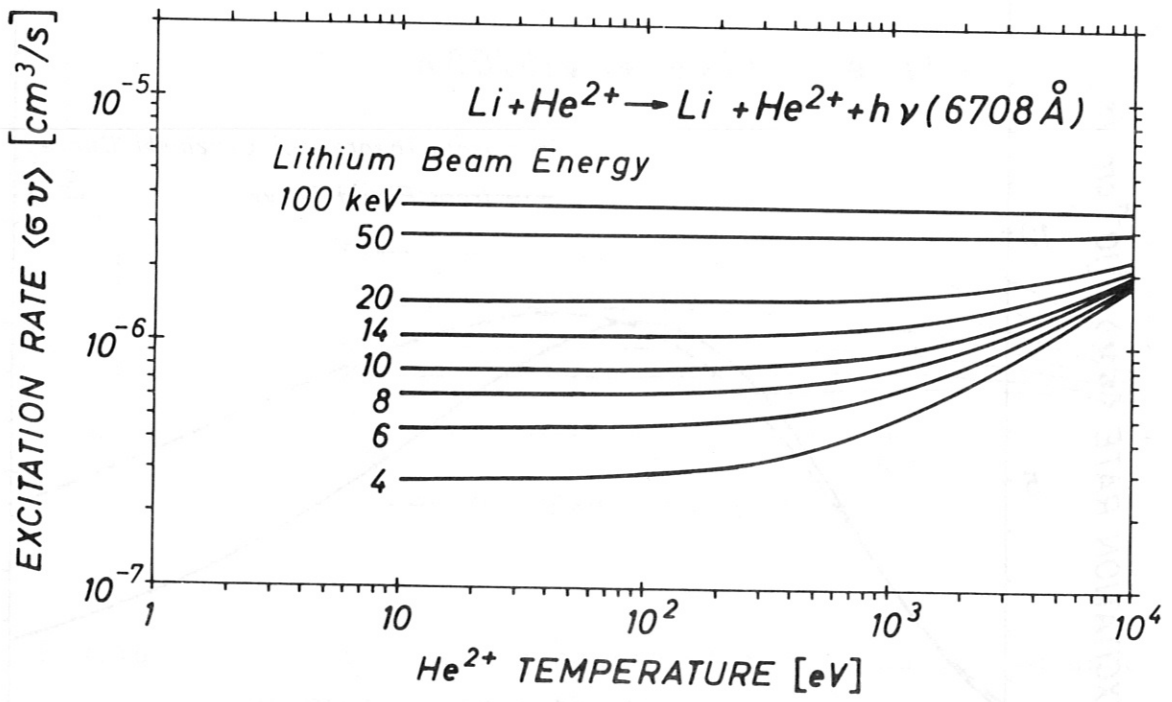

Fig.20 Li(2s-2p) excitation rate for He^{2+} with lithium beam energy as a parameter.

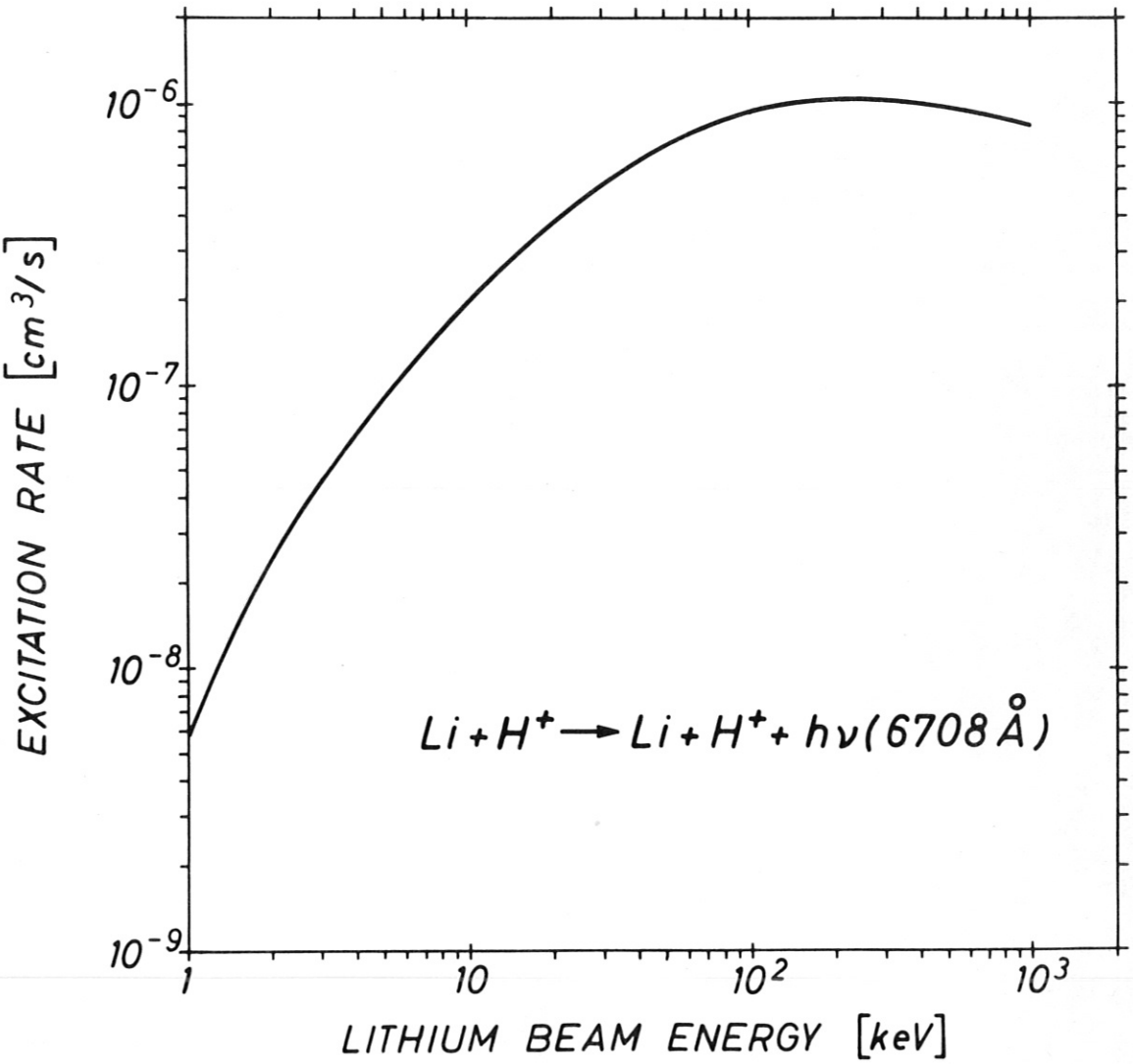

Fig.21 Li(2s-2p) excitation rate for protons as a function of lithium beam energy.